Hydraulic Tomography and High-Resolution Slug Testing to Determine Hydraulic Conductivity Distributions – Year 1

The University of Kansas
Department of Geology
and
Kansas Geological Survey*
Brett R. Engard
Carl D. McElwee
John Healey*
Rick Devlin

Kansas Geological Survey
1930 Constant Avenue
Lawrence, Kansas 66047
Open File Report #2005-36

Annual Report
SERDP
Strategic Environmental Research and Development Program
Project # ER1367
December 2005

Table of Contents

Background ……..….. 3

Objective ……...……....…… 3

Technical Approach ……. 3

Introduction ……...……...…… 4

Theory ……...…… 14

Methodology

Field Techniques ……..…….……..…. 22

Data Processing …….……...…….… 34

Results for EC Profiles and High Resolution Slug Testing ……..……. 42

Continuous Pulse Test (CPT) Results ……...….. 47

Summary and Conclusions ……..……..……..…... 54

References …….……...…..... 59

Appendices

A. EC and HRST K Profiles ……..…….……...…….… 62

B. Phase Shift and Exponential (d) Comparison ……..……...…. 69

C. Various K Profile Comparisons for Line Source Data ...…..…. 76

D. Various K Profile Comparisons for Point Source Data ……. 79

E. Technical Publications ……..……....…. 81

Background:

A considerable body of research has shown that the major control on the transport and fate of a pollutant as it moves through an aquifer is the spatial distribution of hydraulic conductivity. Although chemical and microbial processes clearly play important roles, their influence cannot fully be understood without a detailed knowledge of the subsurface variations in hydraulic conductivity at a site. A number of theories have been developed to quantify, in a generic sense, the influence of these variations using stochastic processes or fractal representations. It is becoming increasingly apparent, however, that site-specific features of the hydraulic conductivity distribution (such as high conductivity zones) need to be quantified in order to reliably predict contaminant movement. Conventional hydraulic field techniques only provide information of a highly averaged nature or information restricted to the immediate vicinity of the test well. Therefore, development of new innovative methods to delineate the detailed hydraulic conductivity distribution at a given site should be a very high priority. The research proposed here is directed at addressing this problem by developing techniques with the ability to map 3-D hydraulic conductivity distributions.

Objective:

Since spatial changes in hydraulic conductivity are a major factor governing the transport and fate of a pollutant as it moves through an aquifer, we have focused on the development of new innovative methods to delineate these spatial changes. The objective of the research proposed here is to build on our previous research to develop and improve field techniques for better definition of the three-dimensional spatial distribution of hydraulic conductivity by using hydraulic tomography coupled with high-resolution slug testing.

Technology Approach:

We have been working for a number of years to quantify hydraulic conductivity fields in heterogeneous aquifers. One method we have worked on extensively that shows great promise is high-resolution slug testing. This method allows the delineation of the vertical distribution of hydraulic conductivity near an observation well. We propose to combine this method with another innovative method for investigating the hydraulic conductivity distribution between wells, called hydraulic tomography. We will use an oscillating signal and measure its phase and amplitude through space in order to estimate the hydraulic conductivity distribution of the material through which it has traveled. Our preliminary work has shown that the phase and amplitude of the received signal can be measured over reasonable distances. The high-resolution slug testing results will be used as an initial condition and will provide conditioning for the tomographic inverse procedure, to help with any non-uniqueness problems. Slug test data are most accurate near the tested well and should probably not be extrapolated blindly between wells. Together, slug testing and hydraulic tomography should be more powerful than either one used in isolation and should give the best opportunity to characterize the hydraulic conductivity in-situ by a direct measure of water flow, as an alternative to indirect methods using geophysical techniques.

Introduction

A typical method used to determine fluid behavior in a geologic matrix near a well is a pumping test. Here a pump is installed into a well and groundwater is removed or injected while water levels in surrounding observation wells are monitored. Then the parameters mentioned above can be estimated by monitoring changes in water levels at observation wells at some distance. These types of tests are typically large in scale, (Schad and Teutsch, 1994). Another test is an interference test, which is a special pumping test where the pump discharge has a variable rate. Interference tests are conducted by variable production or injection fluid (hydraulic head changes) at one well, and observing the changing pressure or hydraulic head with time and distance at other locations. These tests are valued to estimate flow characteristics *in situ,* but are measures of the aquifer material over large volumes also.

On the other hand, physical cores of aquifer material can be obtained by a variety of drilling methods. These samples can then be tested in a laboratory (ie. falling or constant head permeability tests) to estimate the hydraulic properties. One advantage to this method is that the sample can be visually inspected. Some disadvantages to this method are that the material is disturbed from its natural environment and the sample is a small representation of the total aquifer.

Another common technique for determining aquifer parameters is to conduct slug tests. A slug test is the addition or extraction of a known volume of fluid to a well while monitoring the response of the aquifer material in order to estimate K. Slug testing is usually only conducted in a single well. It is generally accepted that the radius of influence of a slug test is small and only provides a limited view of subsurface

hydrogeologic properties near the well. Traditionally, slug tests have been initiated with the addition into a well of a known volume of water or a physical slug. More recently, pneumatic methods have become popular (Zemansky and McElwee, 2005; Sellwood, 2001; McCall et al., 2000) for multilevel slug testing. Slug tests in low K formations can take very much longer than in material with high permeability. To overcome this, the fluid column in a well can pressurized and the pressure change with time can be used as a alternative (Bredehoeft and Papadopulos, 1980).

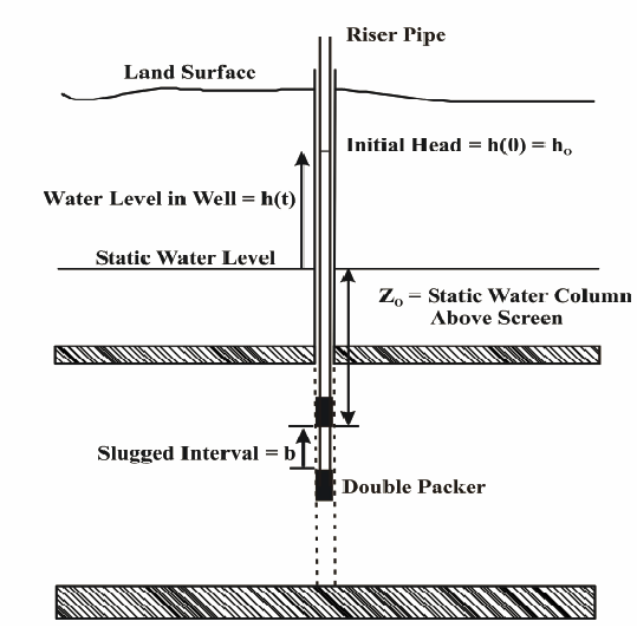

Figure 1. High resolution slug testing equipment deployed in a fully penetrating well.

Typical slug tests are conducted by exciting the entire length of the well screen. Whole well slug testing can provide information near the tested well but it is averaged over the total length of that well's screen. However, aquifers are naturally heterogeneous and whole well slug testing is unable to distinguish areas of high or low K. High resolution slug testing [(HRST), over short screen intervals (Figure. 1)] was developed to provide a more detailed vertical profile of K near the tested well. In this research the

HRST interval is approximately 0.5 m; but, stressed intervals as small as 5 cm have been used (Healey et al., 2004). Currently there is no accepted method to bridge the gap between the larger lateral well-to-well averages from pumping or interference tests and detailed vertical estimates of K from HRST. Proposed here is a method to obtain estimates of aquifer parameters at larger radii of influence, while simultaneously maintaining a higher resolution.

Pulse testing is one method of determining fluid flow parameters that is often employed by the petroleum industry. Johnson et al. (1966) published results to experiments conducted in a sandstone reservoir near Chandler, OK. It was found that the new pulse method was as effective as typical interference tests. The transient pressure signal is propagated by *in situ* fluid and is therefore a direct measure of reservoir diffusivity. Other advantages of the pulse method are the ability to distinguish the test from background noise because of its controlled frequency of oscillation and the reduction of down time relative to production. Since 1966, pulse testing has been used to delineate fractures (Barker, 1988; Brauchler, et al., 2001) and to predict water flood performance (Pierce, 1977).

The changes in groundwater levels as a result of tidal fluctuations have been well studied (Ferris, 1951) and (Jiao and Tang, 1999). The sinusoidal tidal fluctuations propagated inland through an aquifer are related to aquifer storativity and transmissivity. Solutions to water level fluctuations induced by seismic waves were presented by Cooper et al. (1965). The pressure head fluctuations controlling water levels are a result of the vertical motion of the aquifer but are dominated by dilation of the aquifer porosity. An interference test of alternating oil production and shut in time was conducted to

determine the interconnectivity of wells in a production field (Johnson et al., 1966). Here the source well is assumed to be a line source in an infinite homogeneous reservoir. The time lag and the received amplitude were used to estimate the average well-to-well transmissivity and storage properties of the reservoir. These oil field methods were theoretically adapted to hydrogeologic characterization by Black and Kipp (1981). Analytical solutions of a fracture responding to a single pulse interference test, a slug of water, was modeled and tested by Novakowski (1989). Straddle packers isolated the fracture and were used to apply the slug of water by being deflated. The duration of these tests were on average 30 min. The sequential pumping or removal of water was used to collect head responses between wells (Yeh and Liu, 2000). In these experiments multiple ray paths were analyzed as a hydraulic tomography experiment. Such experiments show promise in their ability to distinguish lateral and vertical 2-D variations in heterogeneity by changes in the signal over the travel path.

The research presented here uses continuous, controlled, sinusoidal pressure signals [the continuous pulse test (CPT)] as a means to estimate vertical profiles of well-to-well averaged hydraulic diffusivity. In this research, the primary method of stimulation of the alluvial aquifer was achieved by pneumatic methods. The column of air within a well was pressurized via an air compressor. A signal generator was used to open and close valves at the well-head allowing air to enter or exit the well. The signal generator produced an adjustable frequency step function, controlling the periodicity of the pulse-testing event. Theoretically, a square wave pressure test is the simplest to conduct because of the instantaneous pressure changes (Lee, 1982). Due to the input air pressure, the water column in a well will be depressed creating flow through the well

screen. This pulse of hydraulic pressure is transferred to the aquifer system based on the diffusivity of the material. As the air column within the well is allowed to return to atmospheric pressure, water will rush back into the well from the aquifer. These fluctuations are periodic and similar to tidal fluctuations acting upon a costal aquifer system. The governing equations for an aquifer responding to tidal fluctuations were adapted to Cartesian, cylindrical, and spherical coordinate systems describing groundwater flow with sinusoidal boundary conditions.

The period, the phase, and the amplitude of the produced wave can then be measured simultaneously at the source well and at observation wells. Through dispersion, the aquifer material will decrease the fidelity of a step input, retard the propagation, and attenuate the propagating wave front, resulting in a phase lag or shift, and a decrease in the amplitude. The amplitude ratio [received amplitude A_r divided by the initial amplitude A_0] and the phase difference [reference phase ϕ_0 minus the received phase ϕ_r] can then be used to calculate the hydraulic diffusivity (Lee, 1982).

Zero Offset Profile (ZOP, source and receiver at same elevation) CPT data were collected at the University of Kansas' Geohydrologic Experimental and Monitoring Site, (GEMS) a well-studied shallow semi-confined alluvial aquifer system in the Kansas River floodplain. Line sources equal to the total screen length and point sources isolated by custom bladder packers were used in these experiments. Field data indicate that sinusoidal signals can propagate reasonable distances, and may provide estimates of the average well-to-well diffusivity. Vertical profiles of hydraulic conductivity (K), measured with high-resolution slug testing (HRST), and bulk formation electrical

conductivity (EC) profiles, measured by direct push methods, were collected for correlation with the CPT data.

The study area is the University of Kansas GEMS area located in Douglas County, northeast Kansas, along the northern margin of the Kansas River flood plain (Figure. 2). GEMS is in a Pennsylvanian bedrock valley filled with Wisconsinan-age glaciofluvial terrace sediments (Schulmeister, 2000). The upper 11 m of sediments are mostly silts and clays and the lower 12 m of sediments at GEMS consists of a fining upward sequence of pebbles, coarse sand, and fine sand, which is underlain by the Tonganoxie Sandstone (Jiang, 1991). Within the sequences of sandy material are lenses of low permeability fine-grained sediments. These clay lenses occur at various elevations and can be up to 1 m thick (Schulmeister, 2000 and Healey et al., 2004). As an aquifer, the Kansas River alluvium is a prolific deposit of unconsolidated sands and gravels. It is a high yielding semi-confined aquifer meeting the needs of agricultural, industrial, and community interests.

Many studies have been conducted at GEMS and many well nests have been completed to various depths with various screen lengths. Porosity, grain size, and laboratory K calculations were performed by collecting physical samples of the aquifer material (Jiang, 1991). A single well injection tracer test was used to estimate a K distribution by monitoring the transport of an electrolytic solution (Huettl, 1992). The K distribution in an area of GEMS was also estimated by conducting an induced-gradient tracer test through a multilevel groundwater sampling well field (Bohling, 1999). Direct push bulk electrical conductivity (EC) profiling (Figure 3) and direct push pneumatic slug tests were also done adjacent to the tracer experiment well field (Sellwood, 2001).

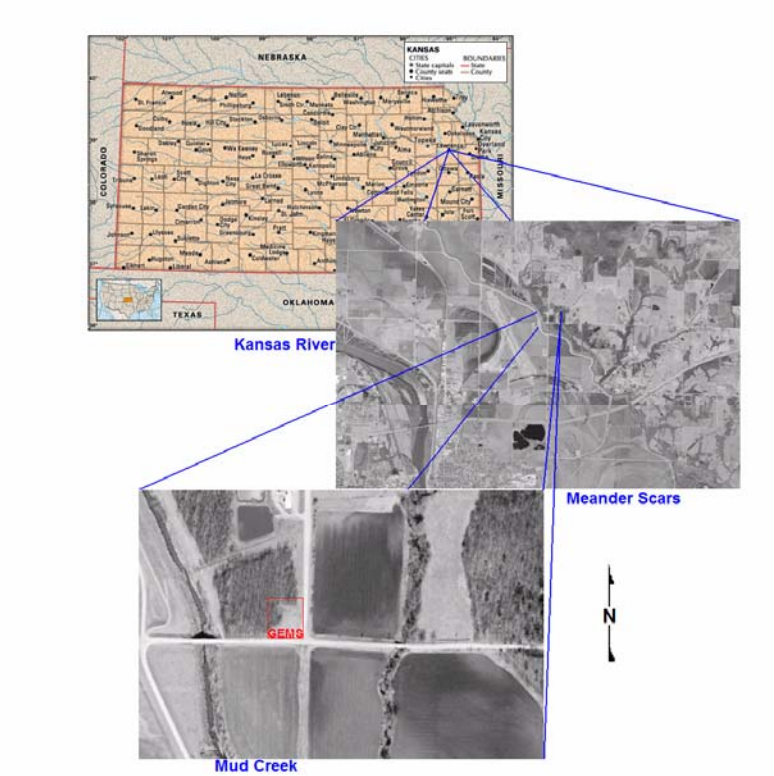

Figure 2. GEMS location map and aerial photographs.

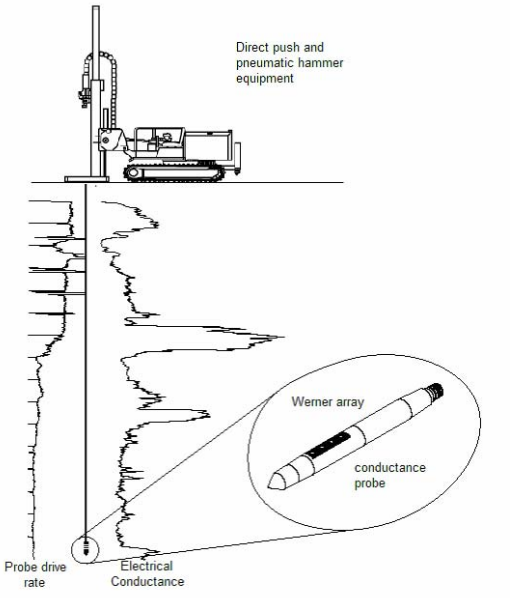

Figure 3. Direct push drilling unit, Electrical Conductance probe, and example profile.

Most recently, HRST K estimates were collected in numerous wells, which were fully screened through the aquifer material (Ross, 2004). The monitoring well and EC locations used in this project are shown in Figures 5 and 6. Table 1 lists some information about wells used in this research. These independent studies and the research presented here all produced estimates of K that can be collected into a database. After compiling this data, vertical and lateral variations of the K distribution are evident. Typically at GEMS, K increases with depth in the sands and gravels, and low K material can be associated with high EC measurements. In some areas at the GEMS, "layers" or zones of high K material are apparent. The high EC readings are also often laterally continuous.

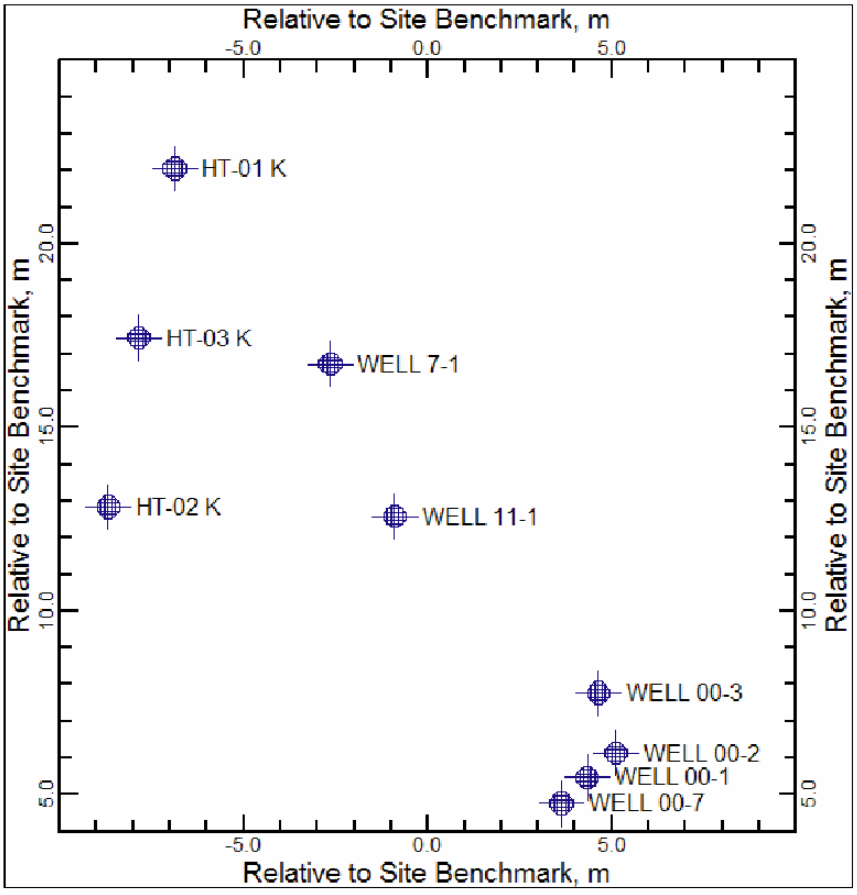

Figure 4 Map of GEMS wells used in this research project

Table 1. Well Information

Location	Elevation ft	Elevation m	Depth ft	Depth m	Screen ft	Screen m
Corps Stake	827.556	252.304	-----	-----	-----	-----
HT-1	829.946	253.032	73.290	22.345	30.0	9.14
HT-2	829.576	252.920	72.670	22.155	30.0	9.14
HT-3	829.000	252.744	69.000	21.037	30.0	9.14
7-1	828.416	252.480	68.850	20.991	30.0	9.14
11-1	828.306	252.532	64.400	19.634	45.0	13.72
00-1	828.823	252.690	55.900	17.043	2.5	0.762
00-2	829.115	252.779	14.410	4.393	2.5	0.762
00-3	828.774	252.675	70.370	21.454	30.0	9.14
00-7	828.958	252.731	66.730	20.345	2.5	9.14

Well to Well Radial Distrances, r

Well	to Well	Distance, r m
00-3	00-2	1.52
	00-1	2.32
	00-7	3.62
	11-1	7.26
	7-1	11.5

Well	to Well	Distance, r m
HT-2	HT-3	4.36

Well	to Well	Distance, r m
7-1	11-1	4.51
	HT-3	5.14
	HT-1	6.44
	HT-2	6.91

Well	to Well	Distance, r m
HT-1	HT-3	4.76
	HT-2	9.13

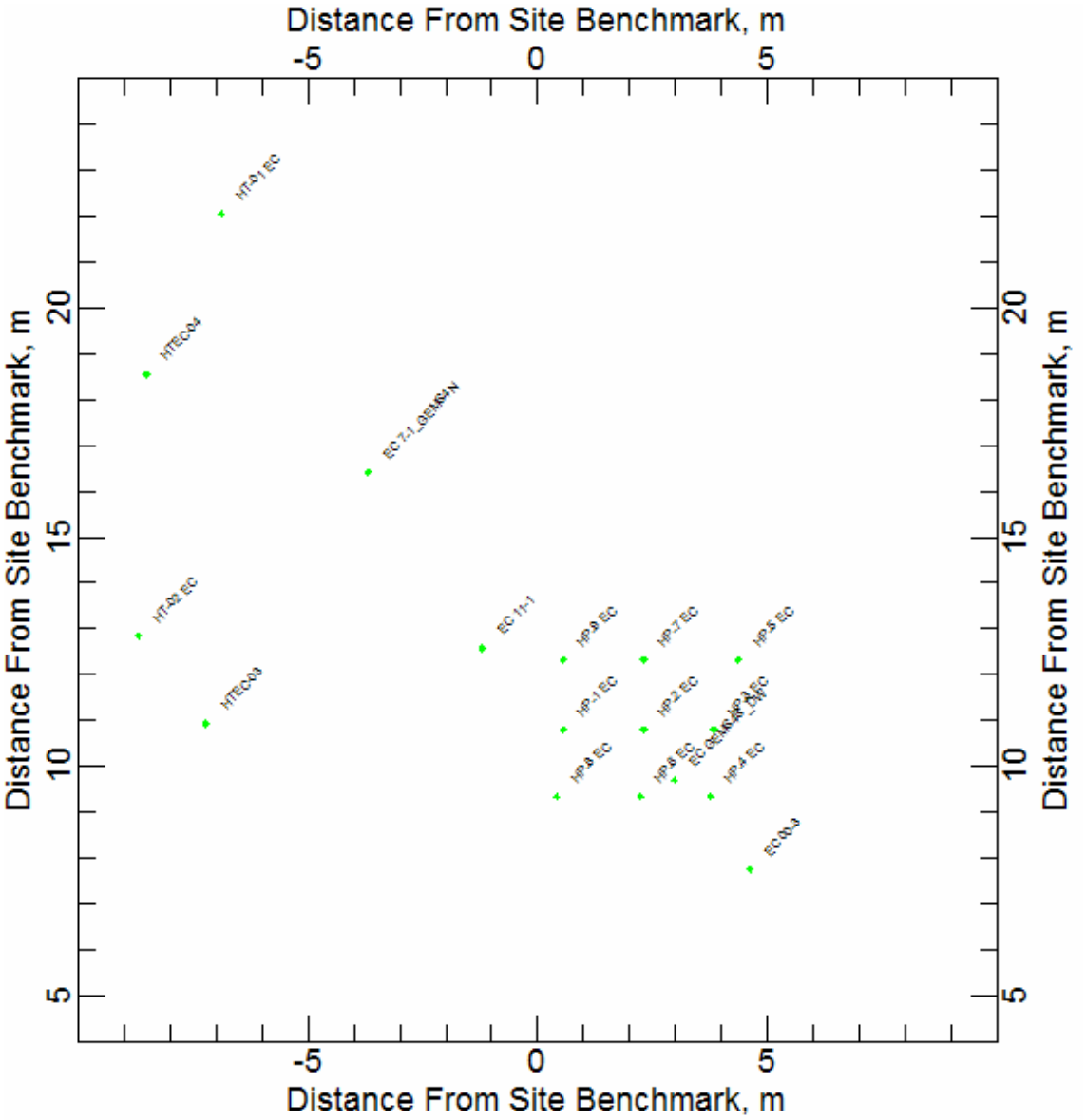

Figure 5. Locations of electrical conductance profiles at GEMS used in this research project.

Theory

Fluid flow in saturated aquifers behaves much like heat flow and can be described by similar equations. Excess pore pressures, matrix permeability, compressibility, and storativity all influence the fluctuations of groundwater levels in response to applied stresses. The excess fluid pressure P_e, above hydrostatic pressure P_s, is related to the total stress on the aquifer σ, and changes the stress $\Delta\sigma$ by

(1) $$\sigma + \Delta\sigma = \sigma_e + (P_s + P_e)$$

The above equation allocates the additional stress to either the aquifer matrix itself or to excess hydraulic pressure, P_e. By changing the hydraulic pressure or hydraulic head, the water levels in an aquifer will also change accordingly. The total hydraulic head (h) hydraulic potential measured in a well is a combination of the elevation head z, and the hydraulic pressure head P

(2) $$h = z + P/\rho g$$

such that

(3) $$P = P_s + P_e$$

Since the elevation is static, the only dynamic portion of h is due to pressure changes as shown in the following equation

(4) $$\frac{\partial h}{\partial t} = \frac{1}{\rho g}\frac{\partial P}{\partial t}$$

where ρ is the fluid density and g is the acceleration of gravity. Substituting equation (3) into equation (9) the total head measured in a well can also be expressed as

(5) $$h = z + (P_s/\rho_w g + P_e/\rho_w g)$$

Darcy's law states that the discharge Q of a fluid through a porous media depends on the hydraulic gradient (the change in head with distance) $\frac{\partial h}{\partial L}$, and the cross sectional area A.

Darcy's Law is

(6) $$Q = -KA\frac{\partial h}{\partial L} \ .$$

Darcy's proportionality constant K, now called hydraulic conductivity, is a measure of how easily a fluid will flow through an aquifer. By combining equation (5) with equation (6) the one-dimensional horizontal flow in the x direction q_x is

(7) $$q_x = -K_x\left(\frac{\partial h}{\partial x}\right) = -K_x\left(\frac{\partial}{\partial x}\right)\left[z + \left(\frac{P_s}{\rho g} + \frac{P_e}{\rho g}\right)\right]$$

Assuming that z and P_s are constant, the flow due to excess pressure is

(8) $$q_x = -\frac{K_x}{\rho g}\left(\frac{\partial P_e}{\partial x}\right)$$

Diffusivity is the ratio

(9) $$D = T/S = K/S_s.$$

D is a measure of the ability of an aquifer to transmit changes in the hydraulic head. The following conservation equations, written either in terms of P_e or h, demonstrate the relationship between K, S_s, and D

(10) $$K_x\frac{\partial^2 P_e}{\partial x^2} = S_s\frac{\partial P_e}{\partial t} \quad \rightarrow \quad D\frac{\partial^2 P_e}{\partial x^2} = \frac{\partial P_e}{\partial t}$$

and

(11) $$K_x\frac{\partial^2 h}{\partial x^2} = S_s\frac{\partial h}{\partial t} \quad \rightarrow \quad D\frac{\partial^2 h}{\partial x^2} = \frac{\partial h}{\partial t}$$

The above equations can be generalized to three dimensions.

It is the goal of this research to utilize the response of hydrogeologic material to cyclic pressure signals to estimate the D distribution in an aquifer.

Groundwater fluctuations near coastal regions have been studied and elementary equations have been developed to associate regional groundwater levels with tidal fluctuations (Hantush, 1960). The basic mathematical description of a one-dimensional transient pressure head signal with sinusoidal boundary conditions [sin(2πft)] is

(12) $$h(r,t) = h_o e^{d} \sin(\Phi_0 - \Phi_r).$$

The head at some distance and time h(r,t) is the initial amplitude h_o, some decay term e^d, multiplied by the sine of the source reference phase ($\Phi_o=2\pi ft$) minus the phase shift, Φ_r. The amplitude decay and the phase shift depend on the ability of the aquifer to transmit the sinusoidal signal. Namely, it is the hydraulic diffusivity (D or K/Ss) of the aquifer which influences the hydraulic head measured at some distance and time from the source of a pressure head fluctuation. Three equations for the head response, within a homogeneous isotropic formation, to the migration sinusoidal boundary conditions, of excess pore pressure, have been adapted from equation (12). Equation (12) has been extended to various coordinate systems, which are presented below.

Linear Cartesian System

(13) $$h(x,t) = h_o e^{-\sqrt{\frac{\pi f S_s}{K}}x} \sin\left(2\pi ft - \sqrt{\frac{\pi f S_s}{K}}x\right)$$

Cylindrical Radial System

(14) $$h(r,t) = h_o \frac{e^{-\sqrt{\frac{\pi f S_s}{K}}r}}{\sqrt{r}} \sin\left(2\pi ft - \sqrt{\frac{\pi f S_s}{K}}r\right)$$

Spherical Radial System

(15) $$h(r,t) = h_o \frac{e^{-\sqrt{\frac{\pi f S_s}{K}} r}}{r} \sin\left(2\pi ft - \sqrt{\frac{\pi f S_s}{K}} r \right)$$

Where t is time, x or r is the distance from the source, f is the frequency, h_o is the initial amplitude of the pressure head fluctuation at the source, S_s is the specific storage, and K is the hydraulic conductivity. Specific storage is the volume of fluid added or released per unit volume of aquifer per unit thickness, from compression or relaxation of the aquifer skeleton and pore due to from changes in stress. The equations (13, 14, and 15) can be thought of as two parts: the amplitude [AMP] on the right hand side

(16) $$AMP = h_o \frac{e^{-\sqrt{\frac{\pi f S_s}{K}} r}}{r^*}$$

where r^* is the respective denominator in equations (13, 14, and 15), and the sinusoidal source phase Φ_o,

(17) $$\Phi_o = \sin\left(2\pi ft\right) \ .$$

The difference in phase Φ_r between two locations is expressed by the term

(18) $$\Phi_r = -\sqrt{\frac{\pi f S_s}{K}} r = d$$

which is equal to the exponential decay term (d) in equations (12, 13, 14, and 15). Both the amplitude decay and the degree of phase shift depend on the ratio of hydraulic conductivity to specific storage, which is the hydraulic diffusivity (D). Estimates of K may be inferred from equation (18) to compare with other methods if S_s is assumed.

The preceding equations can be used to predict phase and amplitude versus distance for homogeneous systems, where K and Ss are constant. However, for

heterogeneous systems where no analytical solutions are available, one must resort to numerical solutions. We postulate that perhaps these relatively simple formulas presented above can be used to analyze the data for heterogeneous cases by using a distance weighted average for the K (hydraulic conductivity) in the above equations. We know from some earlier analytical work that this approach holds some promise for the Cartesian system. It remains to be seen if it can be extended to the cylindrical and spherical cases. The premise is that the following replacement in the above equations might work.

(19) $$\sqrt{\frac{\pi f S_s}{K}}r \quad \Rightarrow \quad \sum_{i=1}^{I}\sqrt{\frac{\pi f S_s}{K_i}}(r_i - r_{i-1})$$

The index (i) indicates the present location of r; so, the summation continues up to the present location of r and terminates at that point.

As indicated above, one must resort to numerical methods to calculate the phase and amplitude relations with respect to distance for heterogeneous cases where K and Ss are changing with distance. We have developed numerical models for calculating the amplitude and phase in the presence of heterogeneity for Cartesian and cylindrical coordinate systems. We have not completed the development for the spherical system yet. In the following section, the results of this numerical modeling for Cartesian and cylindrical coordinates are compared to the simple replacement proposed above to see if it can simplify the inversion for K.

Using the output of the numerical models, we calculated the phase and amplitude as a function of distance for heterogeneous models for the Cartesian and cylindrical coordinate systems. We looked at systems consisting of blocks of material with differing

K and for systems where K varied systematically, such as in a linear trend. As can be seen from the data presented in Table 2, the agreement between the numerical data and the theory using a spatially weighted average to solve for K is excellent, except near boundaries and near the origin. The calculated values for K were determined by

Table 2. Comparison of approximate results for hydraulic conductivity compared with true numerical model values.

Cartesian coordinates:

Two zones for K

x	0	5	10	15	20	25	30	35	40
Amplitude	1	0.333887	0.111552	0.03766	0.010765	0.0046	0.002118	0.000974	0.000449
Phase	0	-0.17316	-0.34662	-0.51784	-0.68759	-0.81992	-0.94258	-1.0656	-1.18951
Cal. K		0.002985	0.002968	0.003198	0.002403	0.005955	0.005943	0.005891	0.005786
True K		0.003	0.003	0.003	0.003	0.006	0.006	0.006	0.006

Linearly varying K

x	0	5	10	15	20	25	30	35	40
Amplitude	1	0.33608	0.126081	0.051371	0.022336	0.010236	0.004895	0.002428	0.001256
Phase	0	-0.16353	-0.3115	-0.44764	-0.5744	-0.69342	-0.806	-0.91361	-1.01703
Cal. K		0.003653	0.004393	0.005133	0.005875	0.006625	0.007354	0.00797	0.008727
True K		0.0036	0.00435	0.0051	0.00585	0.0066	0.00735	0.0081	0.00885

Cylindrical coordinates:

Two zones for K

r	0.0833	1.0231	5.1071	10.0331	15.2399	20.3548	25.4931	30.9181	35.1619	39.9883
Amplitude	1.0000	0.3834	0.0805	0.0200	0.0053	0.0013	0.0005	0.0002	0.0001	0.0000
Phase	0.0000	-0.0494	-0.2012	-0.3753	-0.5565	-0.7248	-0.8690	-1.0028	-1.1080	-1.2289
Cal. K		0.0013	0.0026	0.0029	0.0030	0.0033	0.0045	0.0059	0.0058	0.0057
True K		0.0030	0.0030	0.0030	0.0030	0.0030	0.0060	0.0060	0.0060	0.0060

Linearly varying K

r	0.0833	1.0231	5.1071	10.0331	15.2399	20.3548	25.4931	30.9181	35.1619	39.9883
Amplitude	1.0000	0.3696	0.0766	0.0211	0.0068	0.0025	0.0010	0.0004	0.0002	0.0001
Phase	0.0000	-0.0466	-0.1861	-0.3334	-0.4757	-0.6052	-0.7271	-0.8484	-0.9394	-1.0395
Cal. K		0.0026	0.0035	0.0044	0.0052	0.0060	0.0068	0.0074	0.0081	
True K		0.0031	0.0038	0.0045	0.0053	0.0060	0.0068	0.0076	0.0083	

considering the phases from the numerical models. The results for K using the amplitude data are similar but have a little more error near the origin. We believe this technique

will work for the spherical coordinate system also. We are currently working to verify that. This simplification in solving for K should make the tomographic inversion considerably simpler than if a full numerical model was needed to solve for K.

As shown above, the homogeneous equations can be used to predict K based on the measurable amplitude decay and phase shift. However, the values obtained for the horizontal rays must be interpreted as spatially weighted averages over the horizontal distance between wells. Equations (14) and (15) represent the two experimental approaches utilized in this research. The cylindrical radial equation (14) describes the behavior of the excitation of a relatively long and small radius section of screen and is considered to behave like a line source. Fully penetrating wells are often constructed at GEMS. Any test where the total screen length is excited is termed a whole well test. The spherical radial equation (15) is a representation of the point source geometry, where the excited length of well screen is relatively short. To achieve this, either a partially penetrating well with a relatively short screen length or a straddle packer apparatus must be used. A straddle packer is a double inflatable packer arrangement, which isolates a centralized interval. It would be advantageous if the packer apparatus can be deployed down typical 2 inch (5.08 cm) observation wells; so, considerable effort has been expended to design such packers.

Previous studies have shown that a line source allows for higher energy input, higher amplitudes, and increased signal propagation (Black and Kipp, 1981). A line source can create multiple ray paths to the receiver, decreasing the resolution and only approximating gross K distributions. High K material can also preferentially propagate excess pore pressures generated by a line source, which will induce a vertical gradient

and cross-flow within the aquifer. Depending on the 3-D heterogeneity distribution, this cross-flow will alter the receiver signal, similar to a weighted average, again decreasing the resolution. Even high amplitude line source signals decay rapidly in the subsurface. Most of the decay is due to the exponential term in equations (14 and 15). In addition, the radial distance between source and receiver wells will cause further decay; the cylindrical or line source will additionally decay by the inverse square root of r [equation (14)] and the spherical or point source will decay by the inverse of r [equation (15)]. These additional amplitude decay effects are due to wavefront spreading loss. However, the point source arrangement may increase the resolution of the K distribution profile because of fewer ray path possibilities.

The common component of the amplitude decay and the phase shift is $\sqrt{\frac{\pi f S_s}{K}} r$; therefore, it is possible to compare the phase data to the amplitude data [after correcting for spreading loss]. Using aforementioned assumptions, estimates of K can be obtained through algebraic manipulation. However, this method does not give a specific value for K, but rather an average ratio of S_s/K for the signal travel path from source well to receiver well. Simple theory presented here indicates that the phase and the corrected amplitude ratio should vary linearly with $\sqrt{\frac{S_s}{K}}$ and distance (r) from the source well. Therefore, average parameters between well pairs may be estimated. Further, if multiple source and receiver offsets (relative to their elevations) are used, multiple diagonal ray paths may be recorded. This type of testing is called hydraulic tomography (Yeh and Liu, 2000), and can give more detailed information about hydraulic properties between well. In the first year of this project we have concentrated on horizontal rays where the

source and receiver are at the same elevation (Zero Offset Profiles, ZOP). A ZOP survey is the simplest tomographical survey to conduct and process, but can only give information on average horizontal aquifer parameters.

Methodology

Field Techniques

The field scale distribution of aquifer heterogeneities govern the flow of fluid through alluvial aquifers such as GEMS. In addition, it is these heterogeneities that will dictate the retardation and/or dispersion of a contaminant species in solution with groundwater. Many methods have been developed for the purpose of understanding the dynamic behavior of an aquifer. Recent studies at GEMS have utilized custom-built straddle packers (McElwee and Butler, 1995), and pneumatic slug testing technique techniques [(McElwee and Zemansky, 2000), (Sellwood, 2001) and (Ross, 2004)].

The aquifer material at GEMS exhibits linear and non-linear responses to slug testing (Figure 6). The response of the aquifer material to the slug can be dampened such that water levels in a well return to static head conditions with time in a smooth non-oscillatory curve. However, the aquifer can be underdamped and the water levels will oscillate, decaying with time, until pre-test conditions are reached. Theoretical advances, presented by McElwee and Zenner (1998) and McElwee (2001), have made analysis of nonlinear behavior practical and meaningful. The aforementioned slug tests are localized tests; any correlation between wells separated by some distance must be determined experimentally. Continuous layers of geologic material between tested well pairs should correlate with HRST data from each well in the well pair.

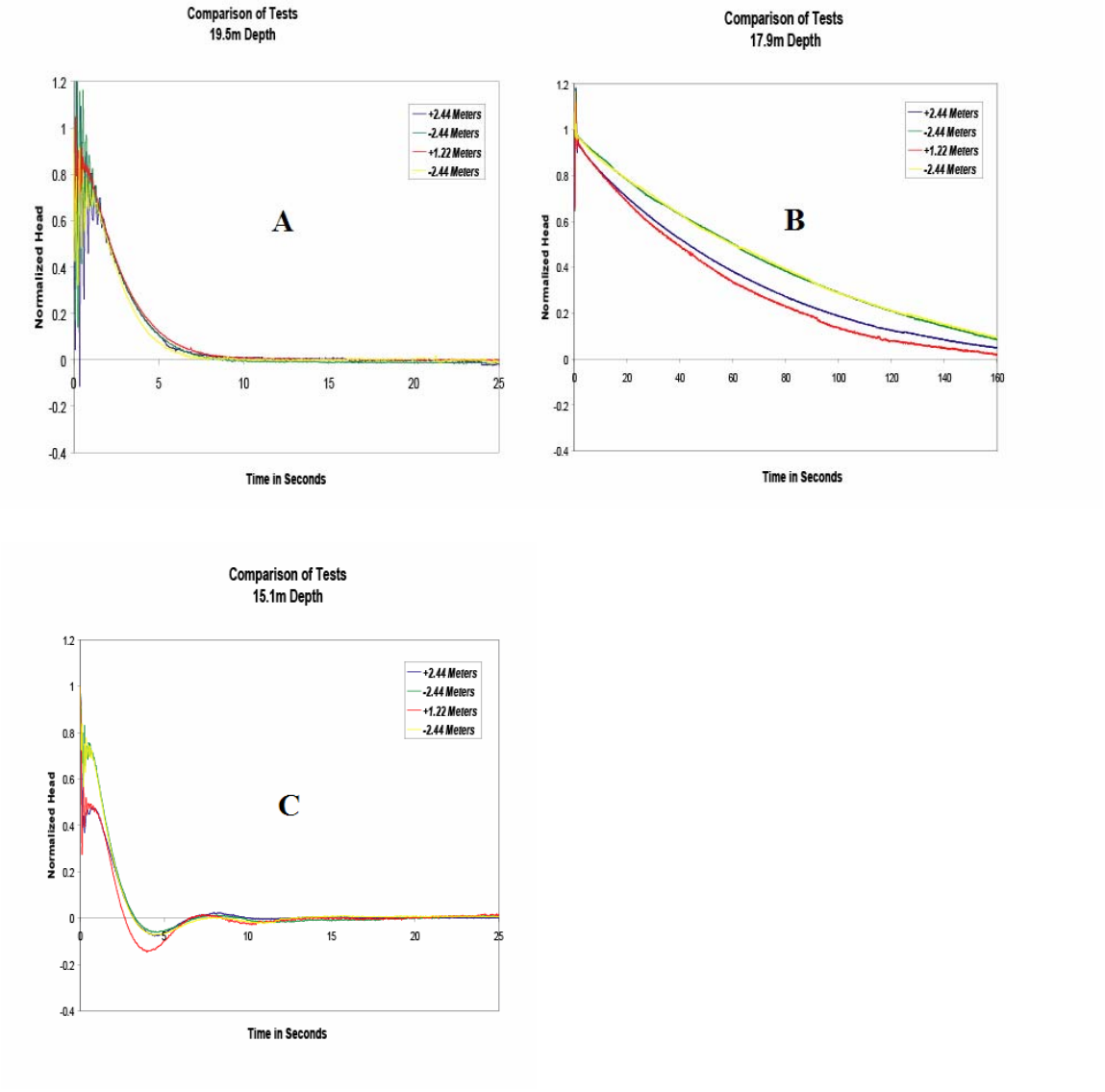

Figure 6. Three examples of slug tests performed at GEMS. Graph A displays no head dependence and behaves linearly. Graph B shows a dependence on the initial slug height and direction. Graph C is oscillatory and has some nonlinear characteristics.

The Continuous Pulse Test (CPT) is an exploratory method for extending slug test results between well pairs by propagating a sinusoidal signal. Well pairs tested and analyzed with the CPT method in this research were between 3 to 11.5 m apart. The instrumentation's ability to discern signal from noise may be a limiting factor at greater

distances. As with most geophysical techniques, the equipment set up time can consume considerable time in the field. The pneumatic CPT method takes slightly longer to perform than the typical high resolution slug test.

Studies have shown that changes in barometric pressure will cause groundwater fluctuations when the well air column is open to the atmosphere (Sophocleous et al., 2004). Therefore, it is possible to move the water column level by changing the pressure in the air column. When the air column pressure is increased or decreased, relative to atmospheric conditions, in time the aquifer water level accommodates the change in air pressure by moving to a new level. The air column is quickly opened to the atmosphere initiating an instantaneous change in head, a slug test. The recovery of the water level is monitored with a pressure transducer and estimates of K can be made.

The continuous pulse test (CPT) was adapted from existing pneumatic slug test techniques and equipment (Figure 7). An air compressor was used to supply the driving force behind the CPT method and it was connected to an apparatus attached to the top of the casing or stand-pipe at the well. A signal generator was used to power servo-controlled valves on the apparatus, which allowed air pressure to be increased in the well or be released to the atmosphere. Increasing pressure depresses the water column, releasing the air pressure allows the water column to rebound. A single pulse of pressure is a slug test, while stacking them one after another, will create a CPT.

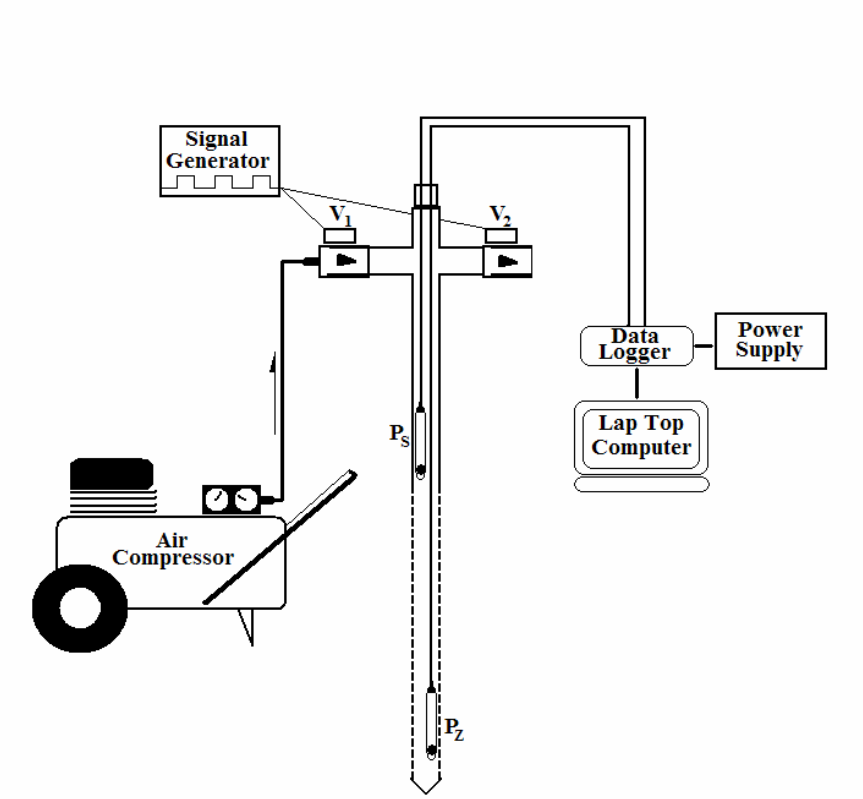

Figure 7. The pneumatic CPT equipment set up for a line source configuration. A signal generator opens and closes valves (V_1 and V_2) to control the flow of air supplied by the air compressor. The pressure transducers record the amplitude and phase at depth P_z and a reference location P_s. This setup can be easily modified for a point source configuration by using a double packer to isolate the stressed interval.

Typically, the aquifer at GEMS has an oscillatory response to whole well slug tests. Both linear and nonlinear recovery of water levels can oscillate about some natural frequency. During preliminary whole well CPT trial, the source wave form was not smooth as expected, but appeared to go through some sort of interference. Whole well slug tests were conducted and the natural frequency of oscillation was determined. When the signal generator's period was not close to the natural frequency of the aquifer, the natural frequency and the induced pressure head fluctuations were out of sync, and would deconstructively interfere. This changes the wave period and alters the shape significantly. The shape of the signal behaves more sinusoidally when the timing of the

signal generator approximates the natural frequency of the aquifer (Figure 8). Albeit this was not an exact process; and within a limited range, the period could be adjusted without significantly sacrificing the wave shape. An adjustable valve was used to restrict the effluent air flow in hopes of improving the sinusoidal signal; but, it did not significantly help. The pneumatic CPT method has an amplitude range limited by the height of static groundwater level above the top of the open screen. Too much amplitude and air would be injected into the formation, potentially changing the aquifer characteristics. Therefore a balance between the influent air pressure, the period of oscillation and the available amplitude excitation range needed to be maintained.

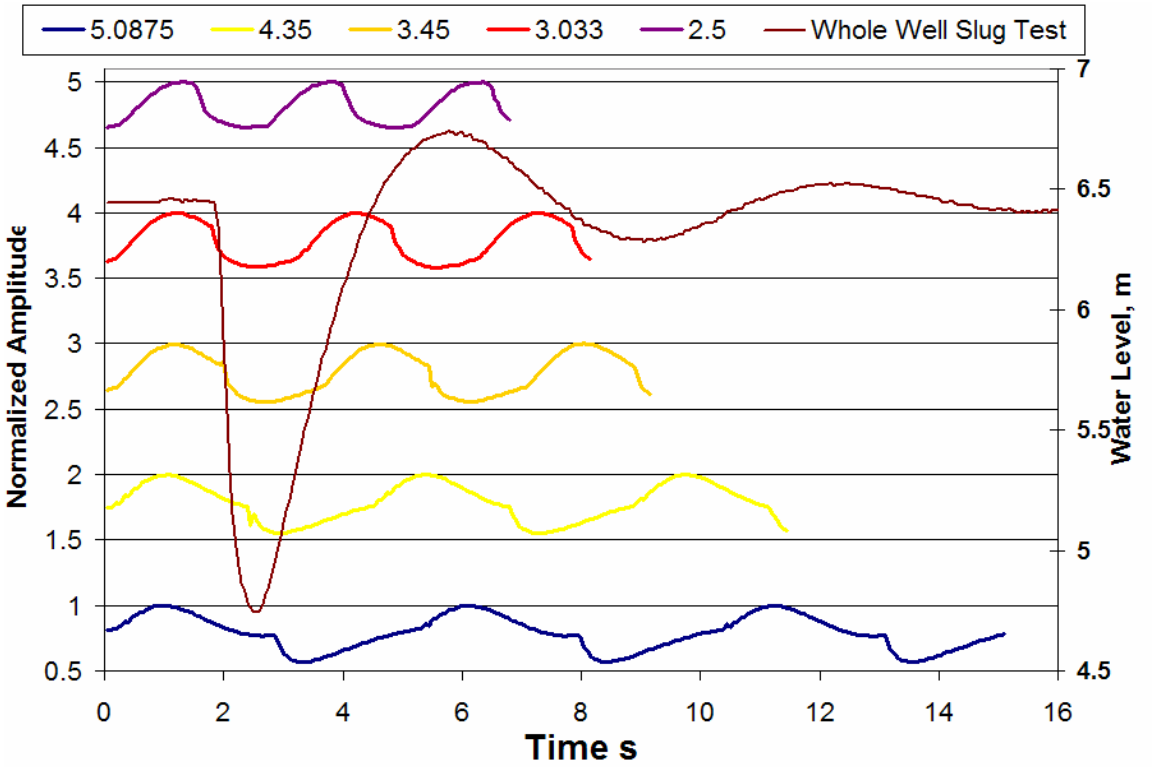

Figure 8. This figure illustrates how the wave form changes as a result of tuning the period of oscillation to the natural frequency of the slugged response in a fully penetrating well at GEMS.

Also during preliminary data collection, the water columns in observation wells were allowed to oscillate freely or they were packed off confining the water column. The oscillating well water column deconstructively interfered with the received signal (Figure 9, source 1 and unpacked observation). By restricting the well water column from oscillating, the received signal fidelity was much improved and the amplitude also increased (Figure 9, source 2 and packed observation). The waveforms shown in Figure 9 are not good sine waves and are only shown to illustrate the good fidelity that can be obtained by packing off the observation well. Therefore, to obtain the most accurate results the receiver pressure transducer should be isolated from the well column.

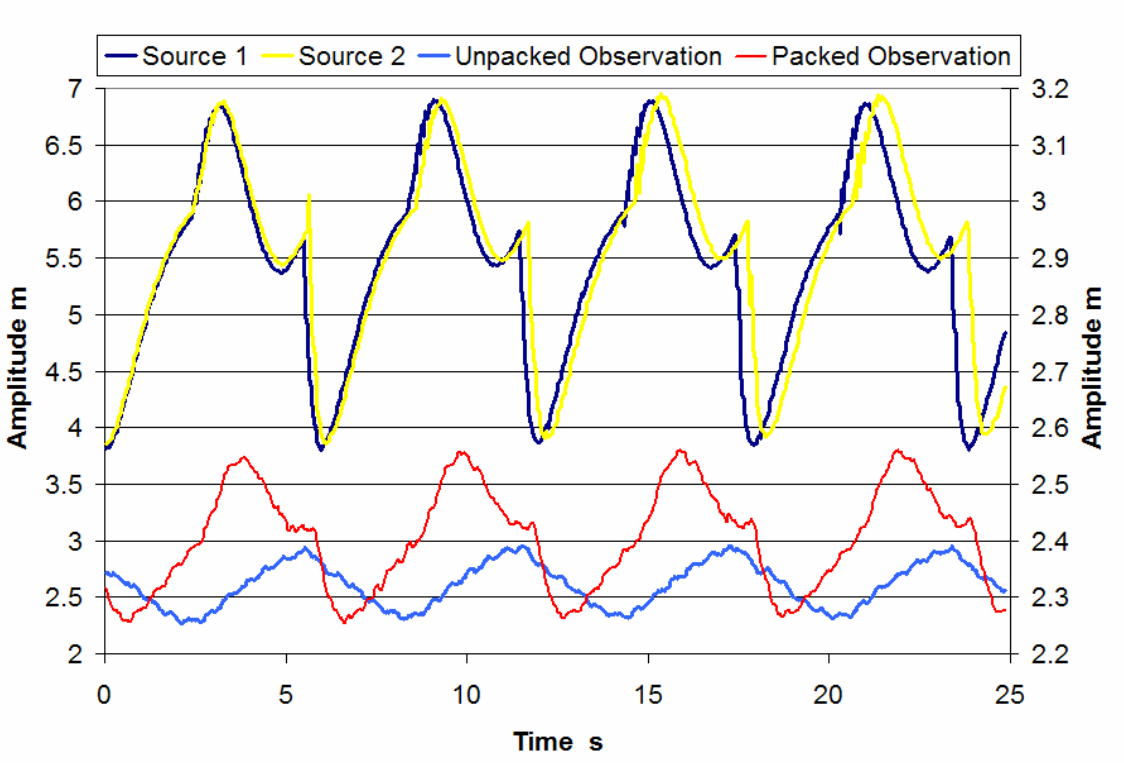

Figure 9. This figure displays the difference between the packed and unpacked response of an observation well.

Some additional experimentation was done to see how the oscillations may be manipulated. The influent air pressure is one of the controls on the amount of producible

amplitude. An increase in the influent pressure increased the source amplitude, the received amplitudes and the propagation distance. Theoretically, longer period waves should attenuate less, increasing the propagation distance. Some experimentation was done with changing the period, but as stated above, there is a narrow range of acceptable differences between the natural period and the driven period. Therefore, only nominal results were obtained before the change in period sacrificed the quality of the wave shape.

There are two geometries in which the CPT was delivered to the aquifer system, a line source and a point source. To produce a line source, the full (~9 m) extent of the source well screen was excited by increasing the head pressure in a source well. Ideally, in a homogeneous aquifer, the excess head pressure will be transferred evenly over the total length of the well screen. The point source geometry applies the excess head pressures over a relatively short section of screen. Although the stressed interval may have a much larger length than the radius, it is assumed that excess pressures will propagate approximately by spherical spreading. The double packer arrangements were custom built so they would have maximum flow-through capabilities; and once inflated, they would block two 0.75 m sections of screen, isolating a 0.5 m interval open to the aquifer. The double packer arrangement could then be raised and lowered to stress different elevations within a fully penetrating well. As employed in a source well, fluid was injected or pneumatically driven into the aquifer through the isolated or stressed interval.

Likewise, the receiver straddle packer could be raised or lowered in the observation well to monitor transient pressures at various elevations in a fully penetrating

observation well. The point receiver apparatus is a way of limiting the influence of multiple ray paths and well storage effects, which should increase the resolution of the method. The receiver double packer arrangement was constructed such that the stressed interval was not in communication with the well water column above or below.

Pressure transducers were used to monitor pressure head fluctuations in both the source well and at the observation wells. The data were collected from the pressure transducers by a data-logger and stored on a field computer for later analysis. Data were typically recorded at a 20 Hz sampling rate, which provided sufficient temporal resolution. The field computer and data logger allowed real-time monitoring of the CPT records. However, during preliminary data collection, off-site high power electrical equipment nearby was producing a noisy electrical environment for recording data with the data logger. The problem was minimized by using a common grounding rod for all the data acquisition equipment. Experiment locations were set by the lowest obtainable elevation common to the source/receiver well pair, referenced to the center of the stressed interval.

A few line source profiles were collected in the next phase of field experiments. The transmitter and the receiver pressure transducers were kept at the same elevation location during the experiments. There was good signal propagation in these experiments; and they had sufficient signal strength to discern the signal from background and instrumentation noise. The recorded field data were processed and fitted to a perfect sine wave. However, when comparing the different locations measured in the vertical profile, the amplitude ratio decreased nearly exponentially and the phase difference increased linearly with depth below the top of the screen. This behavior lead

us to believe that the source signal was not constant in amplitude or phase throughout the total vertical extent in the source well. In previous work by another researcher at GEMS (Huettl, 1992), during a single well tracer injection test the amplitude decayed in a way that was similar to that observed here for the pneumatic whole well CPT data. The amplitude had a linear decay in the well casing due to frictional forces. Once the top of screen was encountered there was non-linear decay from turbulent flow through the well screen and in the aquifer near the well. It seemed that most of the source signal was being input at the upper portion of the screened interval. The Huettl experiments indicated that we needed to investigate how the amplitude and phase changed along the vertical in a whole well CPT experiment.

Experiments were conducted in the source well, using a stationary reference pressure transducer above the well screen and another pressure transducer that was moved to different vertical locations along the well screen. The amplitude and phase in several potential source wells did change with depth and was similar from well to well. The amplitude decreased and the phase change increased with depth (Figure 10).

The amplitude with in the source well decreased nearly exponentially with depth below the top of screen. For example, the amplitude in a source well HT-2 ranged from 1.6 m at the top of the screen to about 0.15 m near the bottom of the screen (Figure 10). The first available open screen would be a preferential exit point for the excess hydraulic pressure of a line source. In addition, the high K material would be the most efficient at accepting the excess pressure induced by the line source. Likewise, when the pressure is released, the high K material should be the dominant influence in water level recovery in the source well. There was also amplitude decay in the well casing above the top of

screen. This additional loss is thought to be a combination of the frictional losses. The most significant amplitude decay is from pressure loss in the screened portion of the well. The phase difference ranged from less than 0.02 at the top of the screen, to 0.36 at the screen bottom. The compressibility of water, frictional losses, and the pressure drop within the well screen are all factors that cause this behavior.

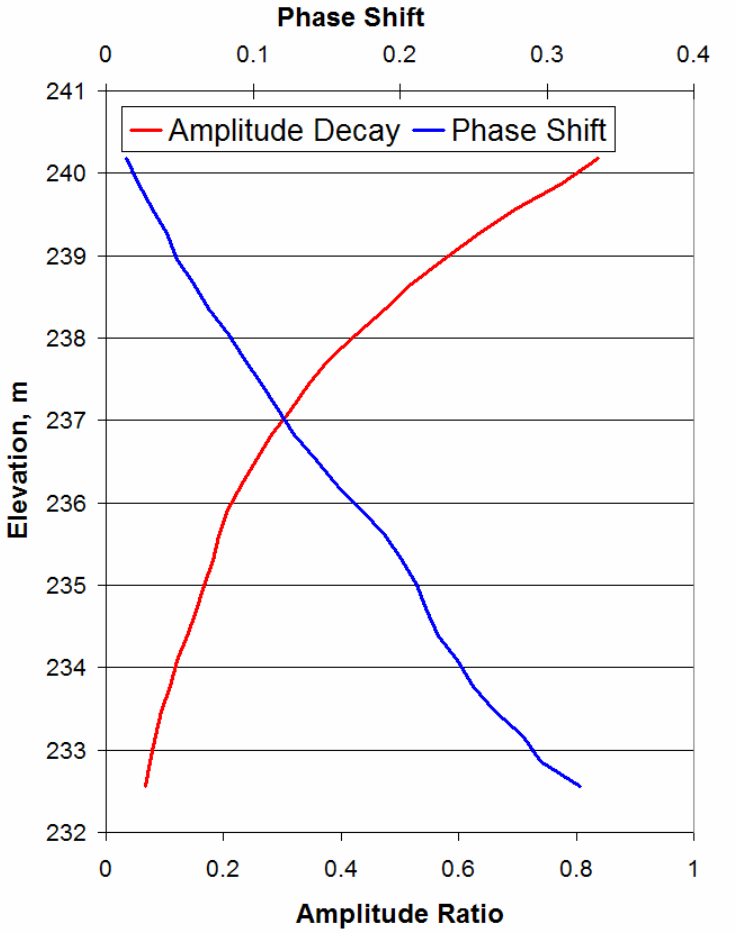

Figure 10. This figure shows the amplitude decay and phase shift along the screened interval in well HT-2 during a pneumatic CPT.

The behavior mentioned above was addressed by making alterations to the experimental procedures and by modifications in the data processing. The following improvements were made to address these factors and collect comparable vertical data profiles. During the line source data collection, at some distance r from the source, a

double packer was used to isolate a receiver in a well, which recorded the amplitude AMP_r and the phase ϕ_r. Two pressure transducers were used in the source well; one was used as a stationary reference location above the top of the screen, to record the amplitude AMP_s and phase ϕ_s. The other pressure transducer was set at the same elevation as the receiver, for each recorded location, and measured the amplitude AMP_z and the phase ϕ_z. The number of recordable ZOP locations depended on the installed screen length and how much of the screened intervals in the well pair overlapped in elevation. Typically about 26 locations were measurable. A profile of the amplitude ratio and phase shift was plotted by converting the locations to depth below top of casing (BTOC) or absolute elevation.

The point source vertical data profiles were collected using two straddle packer arrangements. A double packer with maximum flow-through capabilities was used at the source well; and in a well at some distance r, a double packer was used to isolate a receiver, which recorded the amplitude AMP_r and the phase ϕ_r. Only one pressure transducer was used to record the amplitude AMP_s and phase ϕ_s of the source well at a location near the stressed interval. As with the line source profiles, the recordable locations (about 26) depended on the screen lengths and how much of the screened intervals in the well pair overlapped in elevation. A vertical zero offset profile (ZOP) of the amplitude ratio and phase shift was plotted by converting the locations to depth below top of casing (BTOC) or absolute elevation.

Both the stressed interval of the source well and the isolated receiver interval in the receiver well were about 0.5 m in length. The locations BTOC were referenced to the center of the stressed or received interval. Each location center was approximately 0.3 m

from the next, so that one location overlapped with the adjacent locations. The overlapping intervals acted much like a centered moving average, where the vertical changes in aquifer heterogeneity were averaged over the 0.5 m interval, but were assigned to the center point.

A custom apparatus containing six packers and five pressure ports was built to potentially speed the data collection. The pressure ports were located approximately 1 m apart isolated on either side by packers measuring approximately 0.6 m in length. The main advantage of this apparatus will come when true tomographic surveys are collected, in which multiple variable offset source and receiver locations will be measured. However, the first choice of pressure transducer that was available commercially and sufficiently small was not robust enough. In the first few trials, of the 5 pressure transducers deployed, 3 malfunctioned almost immediately and one failed some time later. We continue to evaluate pressure transducers that may be suitable for this apparatus.

Some non-pneumatic methods for producing a source signal for CPT methods were also evaluated. The first idea was to turn a down-hole pump on and off periodically. Two pumps were evaluated, one for two inch wells and one for a 5 inch well. Both generated signals that could be propagated and measured at nearby wells. However, it is difficult to measure the source signal in the noisy pump environment. Another difficulty with this method is that withdrawing water sets up a water level trend of declining levels. Surge block methods were also tried. The surge block was moved periodically up and down in the well. It produced a reasonably good sinusoidal signal. However, the amplitude was much less than with the pneumatic methods.

We have built an alternate injection system to generate an oscillatory flow signal. It involves pumping at the surface from a reservoir tank to maintain a pressurized water tank. A valve that can be opened and closed at a given frequency is installed in the line going from the pressurized tank on the surface to the aquifer interval of interest below ground, where a valve at the end of the line will be preset to open when the pressure exceeds its cracking pressure. As the valve at the surface opens the cracking valve will open and flow will begin in the aquifer. When the valve at the surface closes the cracking valve will close, shutting off flow and maintaining a line full of water. This will prevent any air from being injected into the aquifer. Initial trials are encouraging, however, it has been hard to find small pressure transducers that are durable enough to measure the injected signal at the packed off interval. It is necessary to have a good representation of the source signal in order to experimentally determine the amplitude ratio and phase difference at the receiver well. We continue to work with this system to produce a cleaner source signal and to measure it more accurately.

Data Processing

The pressure transducers used in routine data collection recorded pressure relative to barometric pressure. A vent tube ran from the surface to the pressure transducer at depth. The generated and received signals were recorded via a data-logger and viewed in real time on a laptop computer during field experimentation. The data logger stored the data on the field computer hard disk as a data file. The raw data could be opened with Excel to inspect for continuity and overall quality. A 7-point moving average filter was applied to all the recorded data to reduce effects of spurious noise in the data. Then, a Visual Basic for Applications (VBA) program FitPhaseAmp, written by Dr. Carl

McElwee, was used to fit a perfect sine wave to the field data (Figure. 11). This program estimated the amplitude, period, and phase. The fitted data were visually inspected to ensure that the program worked well.

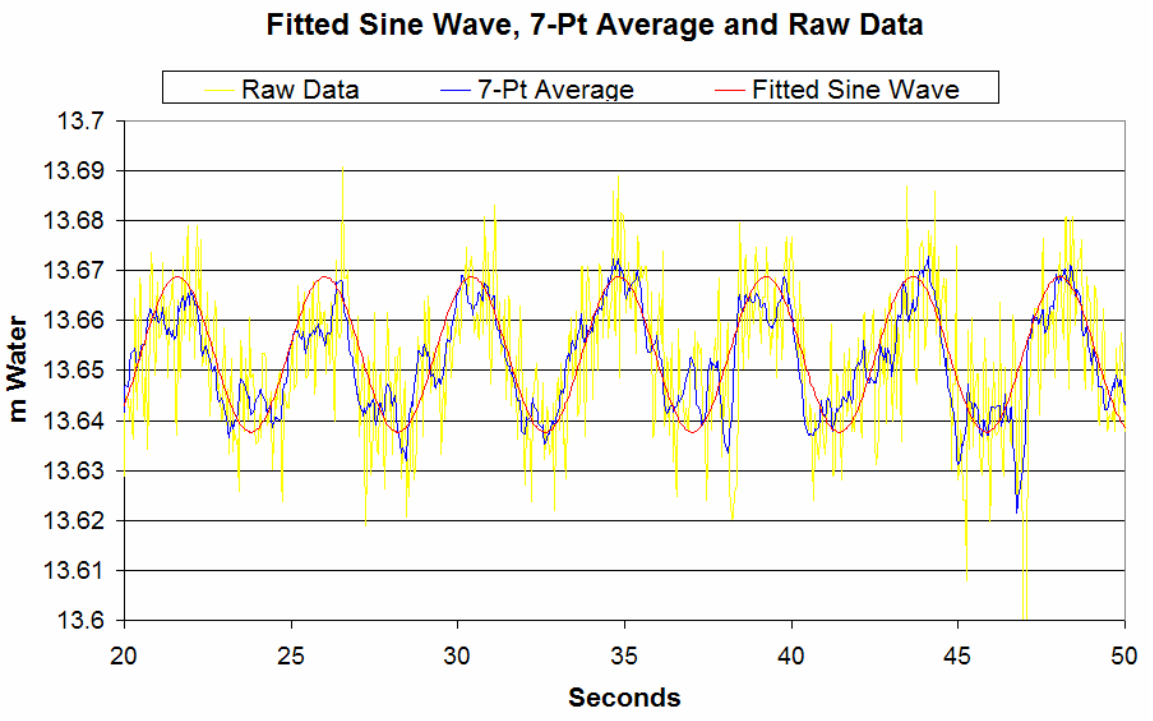

Figure 11. Display of the raw data, raw data filtered with a 7 point moving centered average, and the FitPhaseAmp fitted sine wave of a whole well pneumatic CPT between well HT-3 and 7-1.

The next step was to compute the ratio of receiver and source amplitude and the phase difference. The source and receiver amplitude and phase data are determined individually for comparison. Theory states that the decay term exponential d in equation (12) is equal to the phase shift Φ_r, equation (18). The phase difference, or phase shift Φ_r, was easily computed by subtracting the source phase from the receiver phase of the fitted sine function. On the other hand, the amplitude data are a little more tedious to work with. The received amplitude divided by the source amplitude gives a ratio of amplitudes. The decay term exponential, d in equation (12), is obtained by algebraic

manipulation and correction for loss. The amplitude decays as the leading edge of the source signal grows in surface area. Therefore the received amplitude data need to be corrected for the radial distance from the source. The mathematical steps to correct for spreading losses are outlined below.

Cylindrical Radial System (2D)

(20) $$h(r,t) = h_o \frac{e^{-\sqrt{\frac{\pi fS_s}{K}}r}}{\sqrt{r}} \sin\left(2\pi ft - \sqrt{\frac{\pi fS_s}{K}}r\right)$$

(21) $$AMP_r = h_o \frac{e^{-\sqrt{\frac{\pi fS_s}{K}}r}}{\sqrt{r}}$$

(22) $$\ln\left[\frac{AMP_r}{h_o}\sqrt{r}\right] = -\sqrt{\frac{\pi fS_s}{K}}r$$

Spherical Radial System (3D)

(23) $$h(r,t) = h_o \frac{e^{-\sqrt{\frac{\pi fS_s}{K}}r}}{r} \sin\left(2\pi ft - \sqrt{\frac{\pi fS_s}{K}}r\right)$$

(24) $$AMP_r = h_o \frac{e^{-\sqrt{\frac{\pi fS_s}{K}}r}}{r}$$

(25) $$\ln\left[\frac{AMP_r}{h_o}r\right] = -\sqrt{\frac{\pi fS_s}{K}}r$$

During well installation, a disturbed zone is created between the well and the aquifer material. The disturbed zone at best is a thin veneer around the well, but it may be variable in thickness. In addition, the amplitude in the source well may not be 100%

transferable to the aquifer matrix via the borehole. Therefore, the effective bore hole radius r_o at the source well is at minimum equal to half the inside diameter of the well. Accounting for the effective borehole radius has a profound effect on the amplitude ratio of the CPT data. The mathematical steps for this adaptation are presented below.

Cylindrical Radial System (2D)

Taking the ratio of amplitudes at r and r_o evaluated by equation 21 and taking the natural log gives

(26) $$\ln\left[\frac{\sqrt{r}}{\sqrt{r_o}}\frac{AMP_r}{AMP_o}\right] \cong -\sqrt{\frac{\pi f S_s}{K}}r \quad ,$$

where $r\text{-}r_o$ has been replaced by r on the right hand side, since r_o is very small in comparison to r.

Spherical Radial System (3D)

In a similar manner, using equation (24) the following result is obtained

(37) $$\ln\left[\frac{r}{r_o}\frac{AMP_r}{AMP_o}\right] \cong -\sqrt{\frac{\pi f S_s}{K}}r \quad ,$$

where $r\text{-}r_o$ has been replaced by r again. The value used for r_o can never be less than the radius of the casing. In this research, the minimum allowable radius was 0.0254 m. Since r_o can never truly be known, r_o was used as an empirical fitting term. It was calculated by comparing the phase and amplitude derived values for the term $-\sqrt{\frac{\pi f S_s}{K}}r$, and minimizing the residual sum of the squared differences. The values obtained for r_o

ranged from 0.0254 to 0.18 m. The rational behind this is that it addresses the questions of the effective borehole radius and the efficiency of signal amplitude transmission from well to aquifer.

Additional considerations needed to be addressed for the line source geometry. In the line source well there were two pressure transducers, one stationary (to record the reference amplitude AMP_s and phase ϕ_s) and another pressure transducer to take measurements at an equal elevation as the receiver (to record the amplitude AMP_z and phase ϕ_z with depth). One pressure transducer, in the observation well at some distance r, recorded the amplitude, AMP_r, and the phase ϕ_r. From preliminary data collection, it was found that the amplitude decays nearly exponentially with depth below the top of the screen and the phase shift changes almost linearly (Figure 10). These effects need to be corrected for as well. The value used for AMP_o (for the line source only) was replaced by a cumulative average of the amplitude (AMP_z) in the source well, from the top of the screen to the ZOP elevation of the receiver location. The phase shift, ϕ_z-ϕ_r, was added with the cumulative average of the phase differences (ϕ_s-ϕ_z) within the source well, from the top of the screen to the ZOP elevation of the receiver location. These steps may take into account the multiple ray paths from a line source and the vertical gradient of the amplitude magnitude over the distances spanning the well pairs. Represented mathematically, these corrections are:

Amplitude Ratio Correction

$$\frac{Amp_r}{Amp_0} \cong \frac{AMP_r}{\frac{\sum_{i=1}^{n} (AMP_z)_i}{n}} \tag{28}$$

Phase Shift Correction

$$\Phi_r = (\phi_z - \phi_r) + \frac{\sum_{i=1}^{n} (\phi_s - \phi_z)_i}{n} \tag{29}$$

The point source phase differences should be directly measurable and need no corrections. On the other hand, as the source was placed at different locations, the measured source amplitude was variable even when the period and influent air pressure was kept constant. The source amplitude AMP_z could be measured in the well at the packed-off source interval. The geologic variations in hydraulic diffusivity D were controlling the amount of signal transferred from the source well to the formation (Figure. 12). The source amplitude remained high in low K materials and was reduced as it was applied in high K material. The low K material had a lower propagated amplitude because, relative to the period of the pressure cycling, it would only diffuse a portion of the amplitude from the source well. On the other hand, the high K material would propagate a higher amplitude signal because it was able to accept the source signal much more readily. As a result, the amplitude in the source well measured at the packed off source interval, AMP_z, was much less than expected for the high K material, because it would dissipate the pressure relatively quickly, not allowing pressure to build. Likewise, the excess pressure in the source well would not be dissipated in the low K material because of the low diffusivity and the relatively short oscillation period.

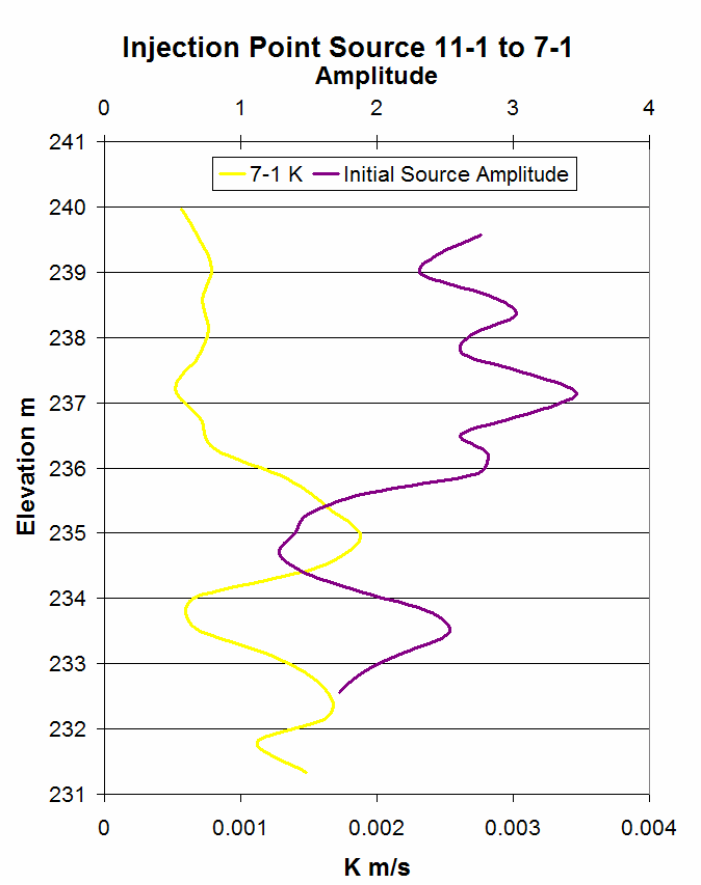

Figure 12. A comparison of the HRST K values of well 7-1 and the point source well amplitude for an injection CPT.

It was assumed that the input amplitude measured at the well screen AMP_z would be sufficient for data reduction. Following the above argument, there is an efficiency associated with the geologic material's inherent ability to transfer the hydraulic pressure from the effective well radius r_o to diffusive flow in the aquifer. To correct for the efficiency of signal transfer from source well to aquifer material, the amplitude ratio is multiplied by a normalization of the source amplitude AMP_z relative to the maximum AMP_z measured. In effect, this is an attempt to back correct for the true AMP_z. However, the maximum recorded source amplitude is sure to be less than the true applied

amplitude AMP_s. Therefore an arbitrary constant (C = 0.30 m of water) was added to the maximum value to estimate AMP_s. Mathematically it is represented by:

Point Source Amplitude Correction

$$\frac{AMP_r}{AMP_s} = \left[\frac{AMP_r}{AMP_z} \left(\frac{AMP_z}{\max(AMP_z) + C} \right) \right] \tag{30}$$

It is assumed that because of the inherent pressure drop with pipe flow, and from flow through the well screen itself, any elevation chosen to record AMP_s would be practically arbitrary. Thus, the maximum value of AMP_z may approximate AMP_s if it is recorded through out the profile at the stressed interval. Similarly, it is critical to measure the phase at the stressed interval because there is a phase shift with depth in the source well.

Making the corrections given by equations (28), (29), and (30) and following the processing procedures outlined previously to obtain equation (26) or (27), the following steps were used to approximate the diffusivity from the final corrected amplitude derived exponential decay term d and the phase shift Φ_r. The frequency was calculated from averaging the reciprocal of the fitted source well period for each CPT. After referring to the literature and calculating an estimate of the specific storage from equation (4), an initial value of 0.00001 was used for S_s (Fetter, 2001; Domenico and Schwartz, 1998). Using a constant value for S_s is unrealistic but is necessary, because even with today's technology, it is difficult to measure S_s *in situ*. The radial distance r can easily be measured in the field or from survey data. With some algebraic manipulation of equation (26) or (27) estimates of K can be made from the CPT experimentally measured phase and amplitude data. The vertical distribution of K was previously measured

experimentally in each well by HRST methods. The HRST K values per well pair for a CPT were averaged together, K^*_{HRST}. Similarly, a mean was calculated from the vertical profile of K calculated using the CPT amplitude (K^*_A) and phase (K^*_P) data. To make the mean CPT K* results ($K^*_{A,P}$) match the mean HRST results (K^*_{HRST}), two ratios C_A and C_P were used. These values were determined by dividing the mean HRST K by the mean amplitude estimated CPT K (C_A) and the mean phase estimated CPT K (C_P).

(41) $$C_{A,P} = \frac{K^*_{HRST}}{K^*_{A,P}}$$

The correction terms, C_A and C_B, were used in an attempt to make the amplitude and phase estimated CPT K values consistent with the HRST K values. In effect, this adjusted the estimate of S_s over the travel distance for each CPT profile. Based on the numerical results presented earlier, the CPT derived values of K should be interpreted as distance weighted averages of K over the path between the source and receiver wells. HRST K values that differ significantly from the CPT K values are evidence of inter-well heterogeneity.

Results for EC Profiles and High Resolution Slug Testing

GEMS is a well-studied site, with approximately 15 years of previous research available through scientific journals, various University of Kansas theses and dissertations, and Kansas Geological Survey (KGS) publications. Two studies used extensively here are University of Kansas masters thesis: “A direct-push method of hydro-stratigraphic site characterization” (Sellwood, 2001), and “Utility of multi level slug tests to define spatial variations of hydraulic conductivity in an alluvial aquifer,

northeastern Kansas," (Ross, 2004). Sellwood performed numerous EC profiles and created a new direct push technique for performing slug tests *in situ* over one foot intervals. His data created a dense grid of EC profiles and K estimates, and can be seen on the location map (Figure 5). Ross used existing wells, extending over the entirety of GEMS, to conduct high-resolution slug testing approximately every 1.5 ft vertical interval in each individual well.

In recent years, direct push technology has proven to be valuable and is receiving attention from scientists and professionals. For shallow groundwater investigations, typical of environmental sites, the relative speed and low cost of direct push applications are more attractive than traditional drilling methods. One tool used with direct push technology is an electrical conductivity (EC) probe (Figure 3). The EC probe outputs a small continuous 5-volt potential and receives the current transported via the material in contact with the probe. Current propagation depends on the characteristics of the matrix material and pore contents. The grain size, packing arrangement, degree of cementation, and mineralogy are intrinsic properties of the matrix, which may affect the EC signal. Most mineral grains are insulators except for metallic ores and clays, which are conductive (Sharma, 1976). Direct push technology can allow the investigator to estimate lithology, delineate some contaminate plumes, obtain groundwater samples, and determine some soil/groundwater conditions as a precursor to more extensive monitoring or remediation activities. The vertical resolution of the tool can be less than 0.025 m, in situ, (Schulmeister et al., 2003) if the specific conductance (SC) variations of formation pore water is small. However, the ability of the tool to distinguish hydrostratigraphic details may be limited.

Geoprobe direct push equipment was used to collect many EC profiles (Appendix A) at GEMS. Typically the EC probe was driven to bedrock or refusal [to advance], about 21 to 22 m below grade. The probe is tapered to ensure a good contact between the electrical array and the aquifer matrix. The EC probe uses four electrodes to conduct in situ measurements of the bulk formation electrical conductivity, in milli-semens per meter (mS/m). The four electrodes allow the probe to be used as a dipole array but a Werner array is the most typical survey arrangement. The resulting measurements can then be displayed in real time in the field on a laptop computer.

Slug testing of an aquifer is an important tool for determining aquifer heterogeneity. Hydraulic conductivity K is a physical measurement of the ability of fluid to flow through a sedimentary deposit or rock. Refinement and advances in well testing techniques have allowed hydrogeologists to better describe a wide range of hydrogeologic settings (Van Der Kamp, 1976; Zurbuchen et al., 2002; and Zemansky and McElwee, 2005). Slug tests have been a common method for obtaining information about the hydraulic conductivity of an aquifer near a well. This type of test will average the hydraulic properties over a limited volume of aquifer. The volume of aquifer tested depends on the length of screen in the aquifer at the tested well. A vertical profile of hydraulic conductivity distributions can be determined using high-resolution slug testing in wells (McElwee, 2000), or even with small diameter direct push equipment (Sellwood, 2001; Butler et al., 2002a,b; McCall et al., 2000). Whole well slug tests use the total, perhaps relatively long, length of the screened interval of a well. High-resolution slug testing enables hydrogeologists to examine vertical variations in K at a much finer scale

relative to whole well slug testing. High-resolution slug testing can be successfully conducted on intervals as small 0.075 m using a double packer arrangement (Figure 1).

The preferred method for initiating a multi-level slug test is to use pneumatics (Zurbuchen et al., 2002). The advantages of using pneumatics are that nothing is added to or produced from the aquifer and less equipment is needed, which is best for contaminated sites. The program NLSLUG (McElwee, 2001) based on the model presented by McElwee and Zenner (1998), was used to aid in the interpretation of oscillatory and non-oscillatory hydraulic head responses from slug testing. The general equation utilized by the NLSLUG program is:

$$(h + z_o + b + \beta)\frac{d^2h}{dt^2} + A\left|\frac{dh}{dt}\right|\frac{dh}{dt} + \frac{g\pi r_c^2}{FK}\left(\frac{dh}{dt}\right) + gh = 0 \quad (43)$$

where β is function of radius changes in the well, A is the nonlinear parameter based on frictional forces and the velocity of the water column, F is the Hvorslev for factor, and K is the hydraulic conductivity (McElwee, 2002).

For this project, high-resolution slug test (HRST) techniques were applied to newly installed wells HT-1, HT-2, and HT-3 after they were properly developed. HRST data from other wells (Ross, 2004) also was used for comparison to continuous pulse tests CPTs. A dual packer arrangement with a 0.5 m interval open to the formation was used. The straddle packer was lowered to the bottom of the well, placing the bottom of the stressed interval 0.8 m above the bottom of the well. In order to observe possible head dependance and repeatability, multiple values for positive and negative initial head conditions were used. The regimen of slugging was as follows; +2.4, -2.4, +1.2, -2.4 m

of head. The slug was applied by adding to or removing air from the well air column; this process adjusts the air column pressure relative to ambient air pressure. The air column and the water column were monitored by pressure transducers and were displayed and recorded in real time. After adjusting the air column pressure, when the conditions within the well returned to equilibrium, a valve was opened to initiate the slug test. The data were recorded for a time period sufficient for data analysis, until pre-test static conditions returned. After the testing was completed at a particular interval, the apparatus was moved to the next location, where it would be held in place by inflation of the bladder packers.

Figure 13 shows, as an example, the EC profile and the HRST profile for K at well HT-2. Appendix A shows similar data for all the wells at GEMS being used in this research project to the present time. High-resolution slug tests performed at GEMS show relatively distinct layers of hydraulic conductivity. There is good correlation with K estimates from other studies conducted previously at GEMS. The EC profiles easily distinguish the overlying silt and clay layer from the lower sand and gravel aquifer at GEMS. Some thin silt or clay layers can be discerned on the EC profiles; these sometimes coincide with lower K on the HRST profiles, but not always. However, thicker clay layers such as in the GEMS East well (Figure A7, Appendix A) are easily correlated with low K on the HRST profile. The EC profiles do not measure K directly; so, they are not directly correlatable to the HRST profiles. Nevertheless, the EC profiles are good reconnaissance tools.

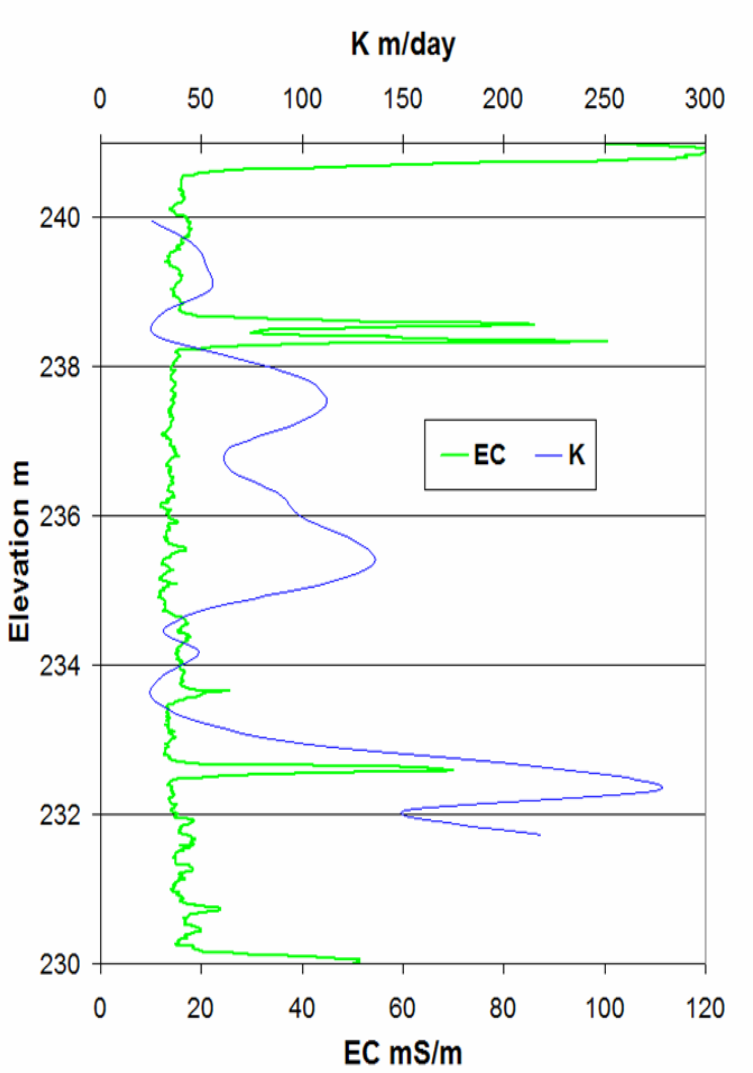

Figure 13. Example of EC and HRST profiles at GEMS well HT-2.

Continuous Pulse Test (CPT) Results

The research presented here uses continuous, controlled, sinusoidal pressure signals as a means to estimate vertical profiles of well-to-well hydraulic diffusivity. The received signal is measured at various depths in observation wells at various distances and locations. The length of the vertical profiles measured by the CPT methods are limited by the amount of open screen common to the well pair in question and by the

length of the bottom packer on the source and receiver double packer apparatus. Typically, the CPT profile was about 8 m in length.

Simple theory (the homogeneous case) predicts that the phase and log amplitude [after correcting for spherical spreading] of the sinusoidal signal should vary with D [ratio of K to specific storage (Ss)] and the radial distance, r, from the source well. The amplitude ratio [received amplitude AMP_r divided by the initial amplitude AMP_0] and the phase difference [reference phase ϕ_z minus the received phase ϕ_r] have both been measured experimentally and used to estimate the spatially averaged D between wells. There are differences in the phase shift and the amplitude derived exponential decay term (d) for the CPT experiments. The simple theory says they should be the same. The amplitude data are probably less reliable because of the exacting experimental measurements that are necessary. Therefore, it was decided that the amplitude derived (d) should be fit to the phase shift by changing the effective borehole radius (r_o). An example of this fitting of d and phase shift is shown in Figure 14 for well pair HT-1 to 7-1. The rest of the results are shown in Appendix B for all the other well pairs for both line source and point source data sets. In general, this procedure brings the two independent data sets into fairly close agreement except for well pair HT-2 to 7-1 (Figure B9, Appendix B). The source of the disagreement in this well pair is unknown at the present time. Using the processing procedures outlined earlier, it is possible to calculate a vertical CPT K distribution from the phase shift data and one for the exponential decay term (d). As outlined in the section on processing, C_A, and C_P are used to make the average of the amplitude and phase derived K distributions equal to the average of the HRST K distribution.

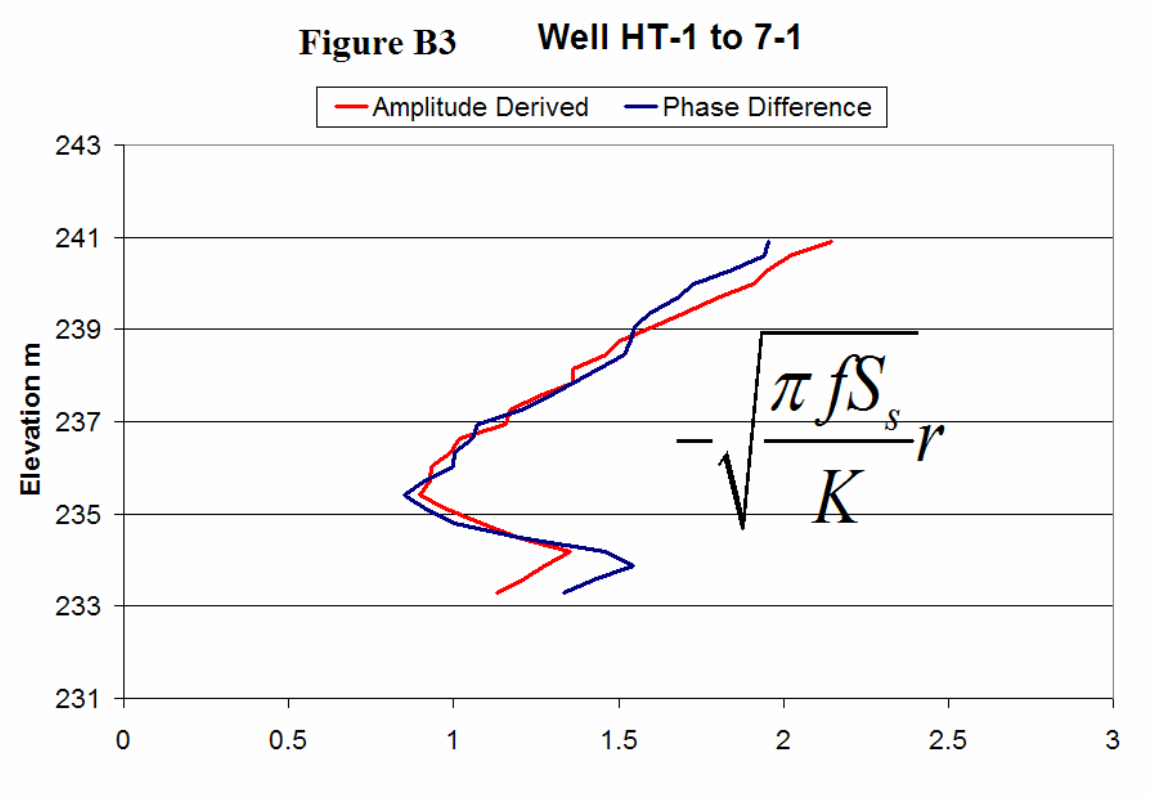

Figure 14. Example of phase shift and exponential (d) agreement after correction for effective radius (r_o)

In total, 7 line source well pairs were tested with the pneumatic CPT method at GEMS. The shortest well separation distance, 4.36 m, was between well HT-2 and well HT-3. For the shortest separation distance, the amplitude ratio ranged between 0.022 to 0.26 and the phase difference ranged from 0.028 to 0.23. The longest separation distance, 11.5 m, recorded was between well 00-3 and well 7-1. For the longest separation distance, the amplitude ratio ranged between 0.004 to 0.017 and the phase difference ranged from 0.01 to 0.4.

Table 3. Line source fitting parameters

Pneumatic Method

Well Pair	r_o	C_A	C_P	Well Distance,m
00-3 to 7-1	0.0254	2.533	1.646	11.5
11-1 to 7-1	0.0306	6.224	6.268	4.51
HT-1 to 7-1	0.0418	3.873	3.924	6.44
HT-1 to HT-3	0.1159	3.183	3.093	4.76
HT-2 to 7-1	0.0442	5.536	5.283	6.91
HT-2 to HT-3	0.0536	4.241	2.633	4.36
7-1 to HT-3	0.0773	9.150	9.186	5.14

In table 3 the values for the fitting parameters r_o, C_A, and C_P for the line source CPT experiments are shown. It is apparent that the radial distance between wells has little correlation with the fitting parameters. The effective borehole radius ranges from the minimum allowable 2.54 cm to 11.6 cm. High r_o values may be an indication of a higher degree of error in measuring the true experimental amplitudes. The fitting program does not allow r_o values less than 2.54 cm, since that is the radius of the casing. The C_A and the C_P parameters for each individual well pair CPT test are in reasonably good agreement, which means that the phase and amplitude data are similar. Therefore, taking an average of the phase derived and amplitude derived K distributions to compare with the HRST K distribution is reasonable. A comparison of the phase derived K distribution, amplitude derived K distribution, and average CPT K distribution compared to the HRST K distribution is shown in Figure 15 for well pair HT-2 to HT-3. Similar profile results for the 7 well pairs that used the line source CPT technique are presented in Appendix C.

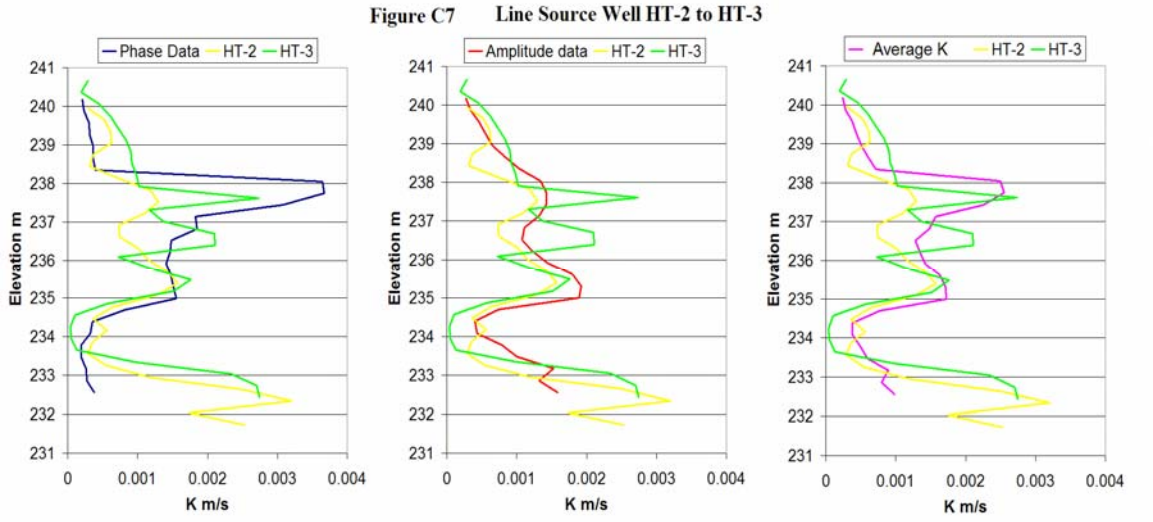

Figure 15. Example of phase, amplitude, and averaged K profiles from line source data compared to HRST K profiles.

Five point source profiles were completed at GEMS with the pneumatic CPT method. Also, one point source profile was completed with the injection CPT method. The shortest well separation distance of 4.36 m was between well HT-2 and well HT-3. For the shortest separation distance, the amplitude ratio ranged between 0.005 to 0.03 and the phase difference ranged from 0.045 to 0.17. The longest separation distance, 6.91 m, was recorded between well HT-2 and well 7-1. For the longest separation distance, the amplitude ratio ranged between 0.0023 to 0.014 and the phase difference ranged from 0.055 to 0.24. The amplitude ratio of the point source data is typically significantly less than the line source data. The phase data are relatively unaffected by the difference in source geometries.

Table 4. Point source fitting parameters

Pneumatic Method

Well Pair	r_o	CA	CP	Well Distance,m
11-1 to 7-1	0.0360	0.519	0.473	4.51
HT-1 to HT-3	0.0470	0.694	1.059	4.76
HT-2 to 7-1	0.0254	12.369	1.378	6.91
HT-2 to HT-3	0.0528	1.545	1.954	4.36
7-1 to HT-3	0.0765	1.153	1.411	5.14

Injection Method

11-1 to 7-1	0.0677	1.334	1.004	4.51

In table 4 the values for the fitting parameters r_o, C_A, and C_P for the point source CPT method well pairs are shown. Again, it is apparent that the radial distance between wells has little correlation to the fitting parameters. The C_A and the C_P terms for each individual well pair CPT test are generally in agreement except for HT-2 to 7-1. This is unexplainable at this time, but is probably related to difficulties in measuring the true amplitudes. A comparison of the phase derived K distribution, amplitude derived K distribution, and average CPT K distribution compared to the HRST K distribution is shown in Figure 16 for well pair HT-2 to HT-3. Similar profile results for the 6 well pairs that used the point source CPT technique are presented in Appendix D.

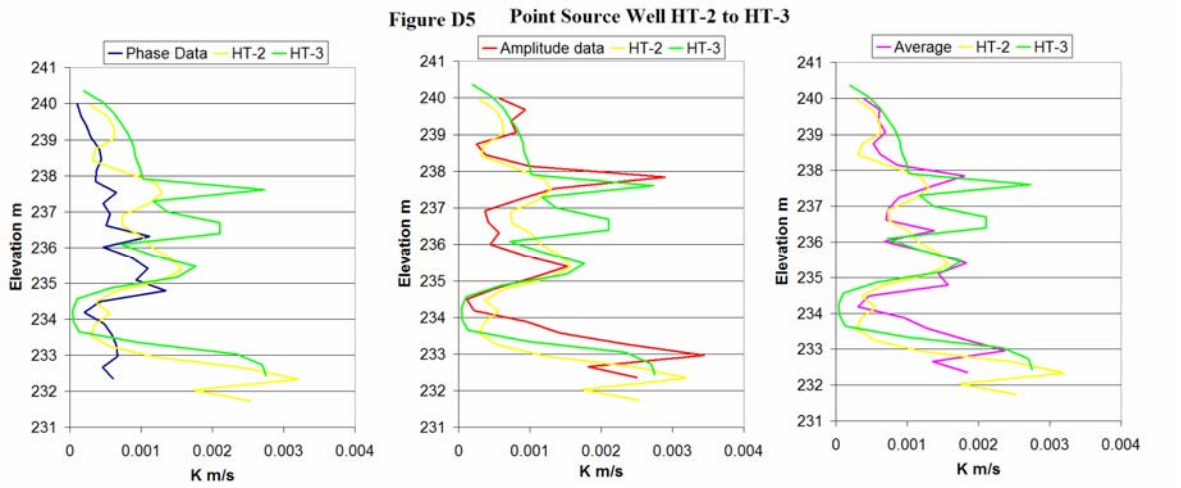

Figure 16. Example of phase, amplitude, and averaged K profiles from point source data compared to HRST K profiles.

It is evident that the CPT profiles mimic the general trends in the HRST K profiles measured at the respective wells (Figures 15 and 16 and Appendix C and D). Overall, the CPT data appear to average the K profiles of the well pair in question. However, there are important differences. On closer examination, the differences in the amplitude and phase estimated K profiles each reflect changes in the HRST K profile that the other does not. As another indication of the importance of the aquifer heterogeneities, sometimes the source well HRST K profile characteristics are more pronounced in the CPT K profile, and sometimes vice versa. The estimated CPT K profiles appear to depend slightly more on the aquifer properties near the source well, but often approximate changes in K near the receiver well that are not present near the source well. The heterogeneities of the geologic material between the well pair are probably the cause of this difference; and the difference can not be fully explained without using more advanced models and numerical solutions. The point source data appear to increase the

resolution of the data, distinguishing variations in K that are not present in the HRST data.

Summary and Conclusions

The primary objective of this phase of the project was to determine the effectiveness of horizontal pulse testing to obtain better estimates of aquifer parameters. To accomplish this goal, several things had to be done. First, a theoretical and a numerical framework was needed to describe the propagation of a sinusoidal signal. Applying the theory to a real field study site required the development of new equipment and field procedures. To analyze the results of field experiments, a processing scheme was developed. The processed data were compared to other geophysical measurements at the test site to look for compatibility and to look for additional information about heterogeneity.

The phenomenon of cyclic loading has been studied in some detail in the literature. There has also been research into using this behavior to estimate hydrogeological parameters. However, little research has been done at the scale presented here. The distinct advantage of using a sinusoidally varying source is that the intrinsic response of the geologic material is measured by the amplitude and phase of the received sine wave. Two types of source geometries were used: the whole well line source and the isolated point source. The line source introduces a greater amount of energy, and therefore has a greater propagation distance than the point source. On the other hand, the point source geometry allows for a better vertical resolution of the aquifer characteristics.

The application of the theory to the field was an evolving process; as the source and receiver equipment was refined, the field procedures needed to be reassessed. The HRST procedures and equipment used by other researchers guided the transition to CPT and made it relatively easier. Many of the equipment items used in CPT were initially borrowed or adapted from previously existing HRST equipment. To make this type of testing readily available to future researchers, the majority of the equipment was put together from "off the shelf" sources. After an experiment was conducted, the equipment could be revamped to suit the particular stratagem of future experiments.

The success of data processing for these experiments depended on the theoretical framework presented earlier. The prediction of groundwater fluctuations from sinusoidal tidal fluctuations was adapted to our local scale experiments. This framework made it possible to estimate the diffusivity (D) of the aquifer material, the ratio the hydraulic conductivity (K) to the specific storage (S_s), from the ratio of measured amplitudes and the phase shift. Two empirical corrections were necessary to complete the data processing and give more meaningful results. The measured exponential decay term (d) was fitted to the measured phase shift by adjusting the effective borehole radius (r_o). This step is thought to compensate for any disturbed zone caused by well drilling methods and for the efficiency of the geological medium in transferring the signal from the source well. The other empirical correction was to normalize the mean CPT estimated K values to the mean HRST K values. In effect, this correction changed the specific storage estimate in the ratio of K/S_s.

The ability of the aquifer to transfer the signal applied at the effective well radius (r_o) to diffusive flow in the aquifer could alter the phase and the amplitude. For example,

the impinging wave front of a seismic wave at an interface will transfer its energy into reflected and transmitted energy. As the transmitted energy is transferred between media with contrasting acoustical properties, the phase and amplitude will be altered. The phase data appear to be a good measure of the diffusivity; the relative changes are in reasonable agreement with HRST K values. Therefore, a better amplitude derived K estimation may be possible by a better understanding how the signal waveform is changed as it is transferred from borehole to aquifer.

Two other types of geophysical measurements are used to correlate with the results of the CPT method. The electrical conductance profiles (ECPs) measured at GEMS are able to discern the boundaries between the Tonganoxie Sandstone, the unconsolidated sands and gravels, and the confining silts and clays. In the absence of significant pore fluid chemistry changes, the EC method may be able to distinguish small scale hydrostratigraphy, such as clay lenses. The other type of geophysical measurement used for correlation is the high resolution slug test (HRST). The HRST methods used here are able to measure the vertical profile of changes in aquifer characteristics near a particular well. HRST data for several wells in an area may shed some light on the stratification of horizontally deposited geologic units by looking at correlations of various K layers between pairs of wells. There is no physical measurement on the aquifer material between the well pair; therefore, it is only possible to make a linear interpolation between two measured wells for HRST data. The CPT method was designed to bridge the gap between HRST measurements made at individual wells. Even without adjusting S_s, the line source and the point source CPT derived estimates of reflect the general trend in hydrogeological conditions measured by HRST methods.

The fidelity of the received signal was much improved when the borehole water column was not allowed to communicate with the receiver pressure transducer. When the energy input to the aquifer reaches an unpacked observation well, some energy is transferred to the oscillating water column. There are two implications here: the energy not transferred to the well column oscillation is preserved as the transient pressure pulse, and the oscillation of the well column will alter the received signal through constructive or destructive interference with the true response. The aquifer response, or lag time from the initiation of the CPT to a measurable received signal, was relatively fast, and the phase shift was never observed to exceed one cycle. At greater propagation distances, the sensitivity and stability of the pressure transducers limits the ability to record a good signal-to-noise ratio.

As detailed in the previous results section, 7 pneumatic line source CPT profiles and 6 point source CPT profiles were completed at GEMS. The line source method was the simplest arrangement to deploy and data could be collected faster from the well pair. To conduct a point source CPT, an additional packer apparatus had to be assembled, deployed, and moved periodically, which increased the field experiment time. Although once set up, the point CPT profile can be completed relatively quickly. The range of radial distances between tested well pairs was 1.5 to 11.5 m. Larger propagation distances are suggested to be possible from monitoring extraneous distant wells during some field experiments.

The data presented here show that the CPT profiles mimic the general trends in the HRST K profiles measured at the respective wells. Overall, the CPT data appear to average the K profiles of the well pair in question. However, there are important

differences. The heterogeneities of the aquifer between the well pair are probably the cause of this difference; and the difference can not be fully explained without using more advanced models and numerical solutions. Both the line source data and the point source data appear to distinguish variations in K that are not present in the HRST data. However, the point source data appear to have the best resolution of the data presented here.

The CPT method shows promise as a hydrogeological tool. The interpretation of the ZOP CPT data presented here is limited to vertical changes in the mean horizontal aquifer parameters, which are assumed to be given by linear interpolation between wells. To obtain more detail on variations between well pairs, hydraulic tomography may be done with techniques similar to those used here for the CPT method. Hydraulic tomography uses multiple vertical offsets between source and receiver locations. It uses an inversion technique to estimate parameters for a 2-D vertical slice of the distribution of aquifer heterogeneities (Yeh and Liu, 2000). Future research on this project will deal with development of numerical models necessary for interpreting tomographical data and collection of appropriate experimental data. However, the ZOP CPT method can be of practical use for discerning changing horizontal flow units. The dominant direction of groundwater flow is typically horizontal, parallel to unconsolidated geologic bedding planes.

References

Barker, J.A., 1988. A generalized radial flow model for hydraulic tests in fractured rock. *Water Resources Research* 24. No. 10:1796-1804.

Black, J.H., and Kipp, K.L. 1981. Determination of hydrogeological parameters using sinusoidal pressure tests: A theoretical appraisal. *Water Resources Research* 17. No. 3:686-692.

Bohling, G.C., 1999. Evaluation of an induced gradient tracer test in an alluvial aquifer, Ph.D. Dissertation, University of Kansas, 224 p.

Bohling, G.C., Zhan, X., Knoll, M.D., Butler J.J. Jr. 2003. Hydraulic tomography and the impact of a priori information: An alluvial Aquifer Example. *Kansas Geological Survey Open-file Report 2003-71*

Brauchler, R., Liedl, R., Dietrich, P., 2001. A travel time based hydraulic tomographic approach. *Water Resources Research* 39. No. 12:1-12

Bredehoeft, J.D and Papadopulos, S.S. 1980. A method for determining the hydraulic properties of tight formations. *Water Resources Research* 16. No. 1:233-238

Butler, J.J. Jr., Garnett, E.J., Healey, J.M. 2002a. Analysis of slug tests in formations of high hydraulic conductivity. *Ground Water* 41. No. 5:620-630

Butler, J.J. Jr., J.M. Healey, G.W. McCall, E.J. Garnett, and S.P. Loheide II. 2002b. Hydraulic tests with direct-push equipment. *Ground Water* 40, No. 1:25-36

Cooper, H.H., Bredehoeft, J.D., Papadopulos, I.S., and Bennett, R.R. 1965. The response of well-aquifer systems to seismic waves. *Journal of Geophysical Research* 70, No. 16:3915-3926

Domenico, P., and Schwartz, F. 1998. *Physical and chemical hydrogeology*. 2nd Ed. John Wiley & Sons. New York, New York.

Fetter, C.W., 2001. Applied Hydrogeology. 4th Ed. Prentice Hall. Upper Saddle River, New Jersey.

Ferris, J.G., 1951. Cyclic fluctuations of the waterlevels as a basis for determining aquifer transmissivity, IAHS *Publ.*, 33, p. 148-155.

Hantush, M.S., 1960. Lectures at New Mexico Institute of Mining and Technology. unpublished, compiled by Steve Papadopulos, 119 p.

Healey, J., McElwee, C., and Engard, B., 2004. Delineating hydraulic conductivity with direct-push electrical conductivity and high resolution slug testing. *Trans. Amer. Geophys. Union* 85, No.47: Fall Meet. Suppl., Abstract H23A-1118.

Huettl, T.J., 1992. An evaluation of a borehole induction single-well tracer test to characterize the distribution of hydraulic properties in an alluvial aquifer. Masters Thesis, The University of Kansas.

Jiang, X., 1991. Field and laboratory study of the scale dependence of hydraulic conductivity. Masters Thesis, The University of Kansas.

Jiao, J.J. and Tang, Z., 1999. An analytical solution of groundwater response to tidal fluctuation in a leaky confined aquifer. *Water Resources Research* 35. No. 3:747-751

Johnson, C.R., Greenkorn, R.A., and Woods, E.G., 1966. Pulse-Testing: A new method for describing reservoir flow properties between wells. *Journal of Petroleum Technology.* (Dec1966) pp. 1599-1601.

Lee, J., 1982. Well Testing. Society of Petroleum Engineers of AIME, New York. 156 p.

McCall, W., Butler J.J. Jr., Healey, J.M., and Garnett, E.J., 2000. A dual-tube direct push method for vertical profiling of hydraulic conductivity in unconsolidated formations. *Environmental & Engineering Geoscience* Vol. VIII, no. 2:75-84

McElwee, C.D., 2001. Application of a nonlinear slug test model. *Ground Water* 39. No. 5:737-744

McElwee, C.D., 2002. Improving the analysis of slug tests. *Journal of Hydrology* 269:122-133

McElwee, C.D., and Butler, J.J. Jr., 1995. Characterization of heterogeneities controlling transport and fate of pollutants in unconsolidated sand and gravel aquifers: Final report. Kansas Geological Survey open file report 95-16.

McElwee, C.D., and Zenner, M.A., 1998. A nonlinear model for analysis of slug-test data. *Water Resources Research* 34. No. 1:55-66.

Novakowski, K.S., 1989. Analysis of pulse interference tests. *Water Resources Research* 25. No. 11:2377-2387

Pierce, A., 1977. Case history: Waterflood perfomance predicted by pulse testing. *Journal of Petroleum Technology.* (August 1977) 914-918.

Ross, H.C. 2004. Utility of multi level slug tests to define spatial variations of hydraulic conductivity in an alluvial aquifer, northeastern Kansas. Masters Thesis, The University of Kansas.

Schad, H., and Teutsch, G., 1994. Effects of scale on pumping test results in heterogeneous porous aquifers. *Journal of Hydrology* 159. pp. 61- 77.

Schulmeister, 2000. Hydrology and geochemistry of an alluvial aquifer near a flood plain margin. Dissertation, University of Kansas.

Schulmeister, M.K., Butler, J.J. Jr., Healey, J.M., Zheng, L., Wysocki, D.A., and McCall, G.W., 2003. Direct-Push Electrical Conductivity Logging for High-Resolution Hydrostratigraphic Characterization. *Ground Water Monitoring & Remediation* 23. No. 3:52-62.

Sellwood, S., 2001. A direct-push method of hydrostratigraphic site characterization. Masters thesis, The University of Kansas.

Sharma, P., 1976. *Geophysical methods in geology*. Elsevier. New York, New York.

Sophocleous, M., Bardsley, E., Healey, J., and Engard, B., 2004. Can precipitation loading be detected at 300-meter depth or greater? Kansas Geological Survey, Open-File Report 2004-46. 19 p.

Van Der Kamp, G.,1976. Determining aquifer transmissivity by means of whole well respons tests: The underdamped case. *Water Resources Research* 12. No. 1:71-77.

Yeh, T.C., and Liu, S., 2000. Hydraulic tomography: Development of a new aquifer test method. *Water Resource Research* 36. No. 8:2095-2105

Zemansky, G.M., and McElwee, C.D., 2005. High-Resolution Slug Testing. *Ground Water* 43. No. 2: 222-230

Zurbachen, B.R., Zlotnik, V.A., and Butler, J.J. Jr., 2002. Dynamic interpretation of slug tests in highly permeable aquifers. *Water Resources Research* 38. No. 3:1-17

Appendix A. Comparison of EC and HRST K profiles for well pairs at GEMS.

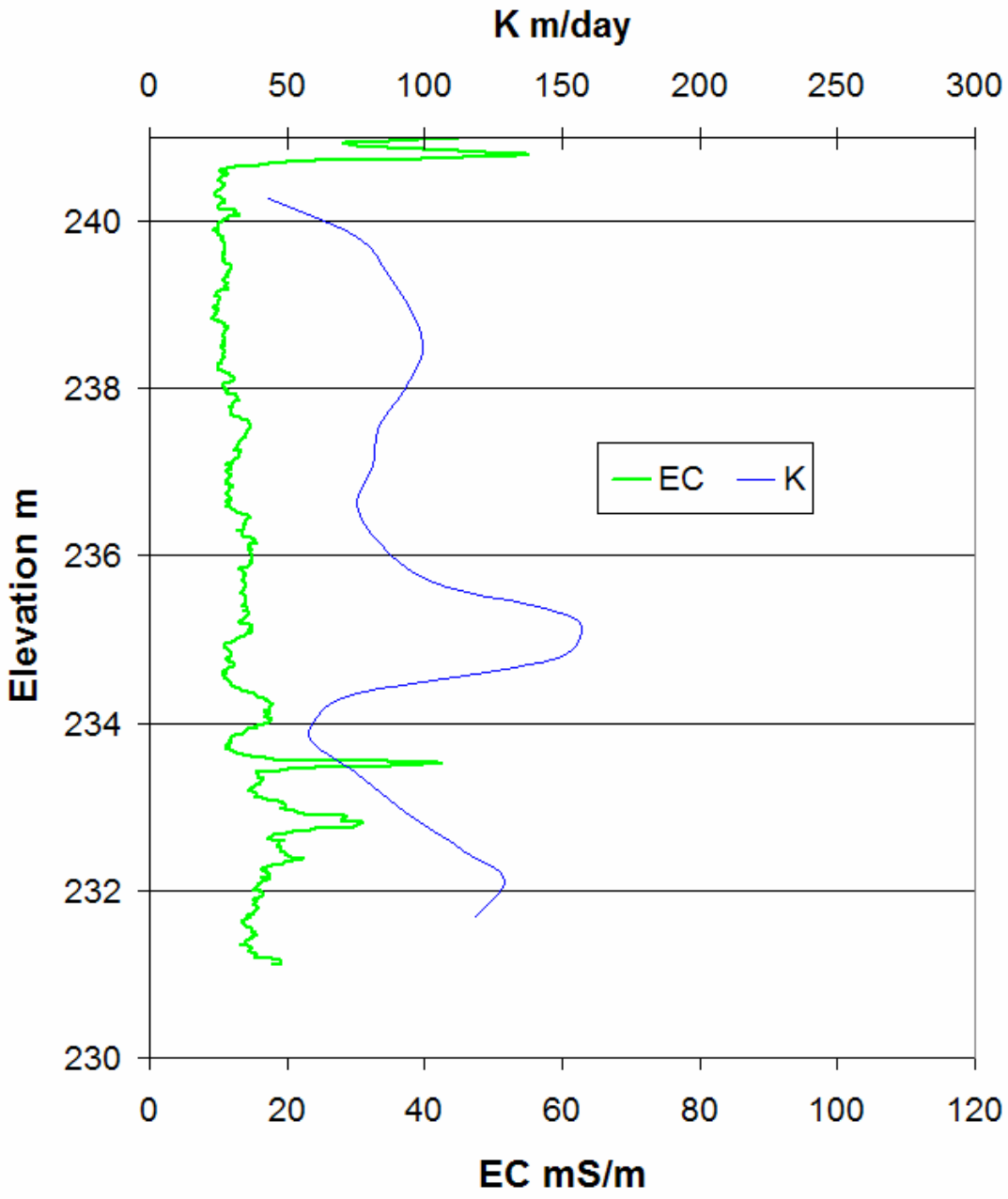

Figure A1. Well 00-3

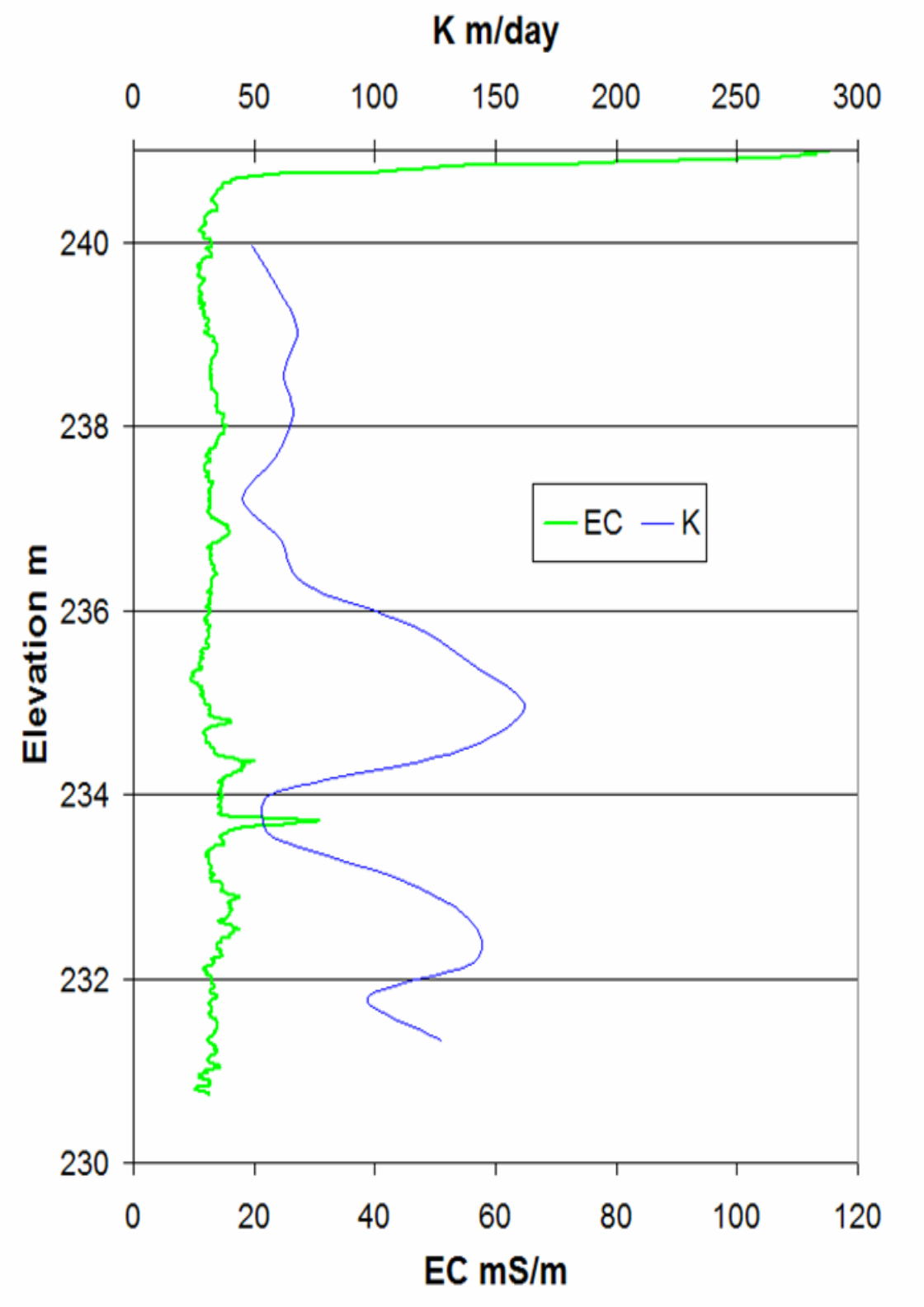

Figure A2. Well 7-1

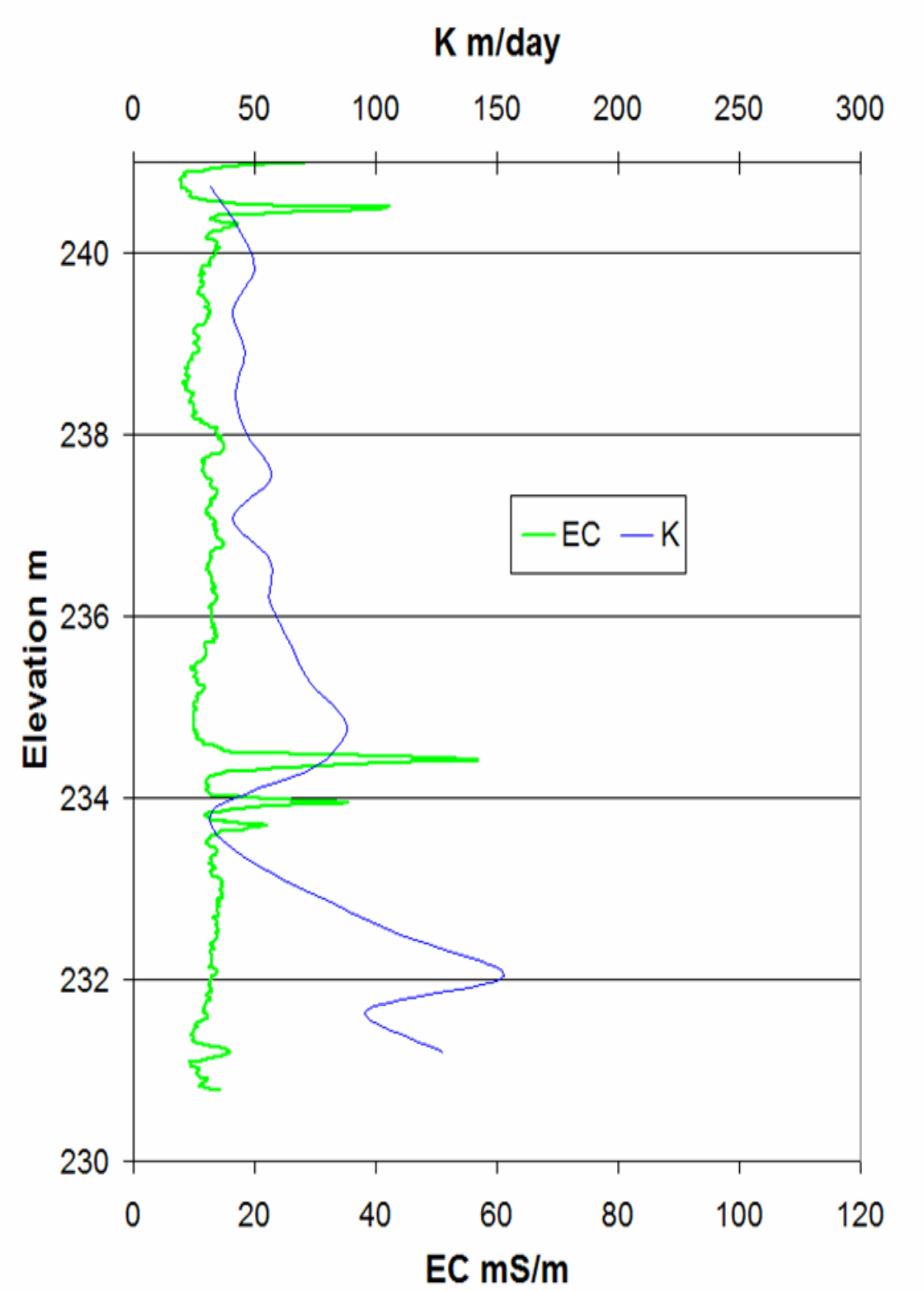

Figure A3. Well 11-1

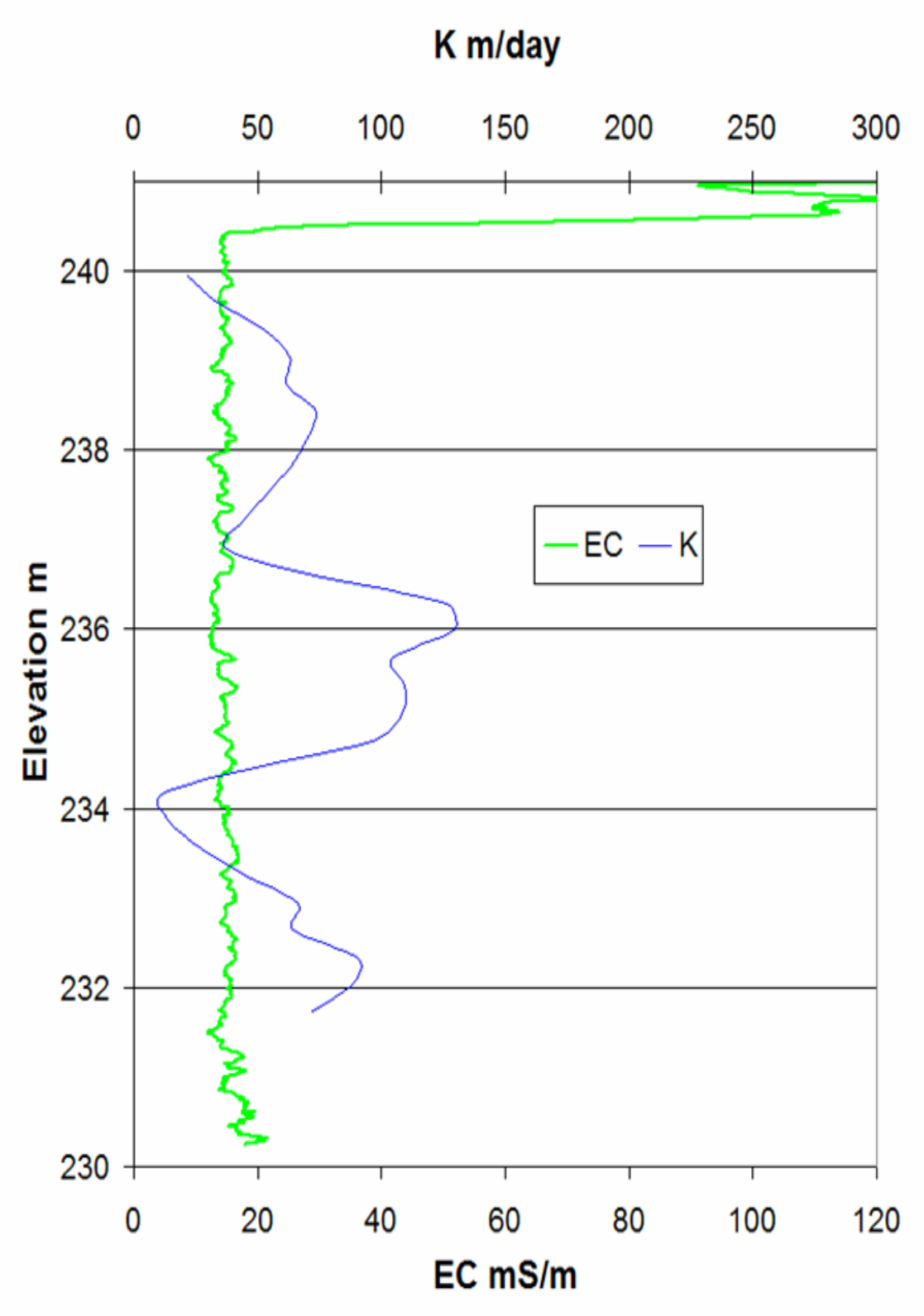

Figure A4. Well HT-1

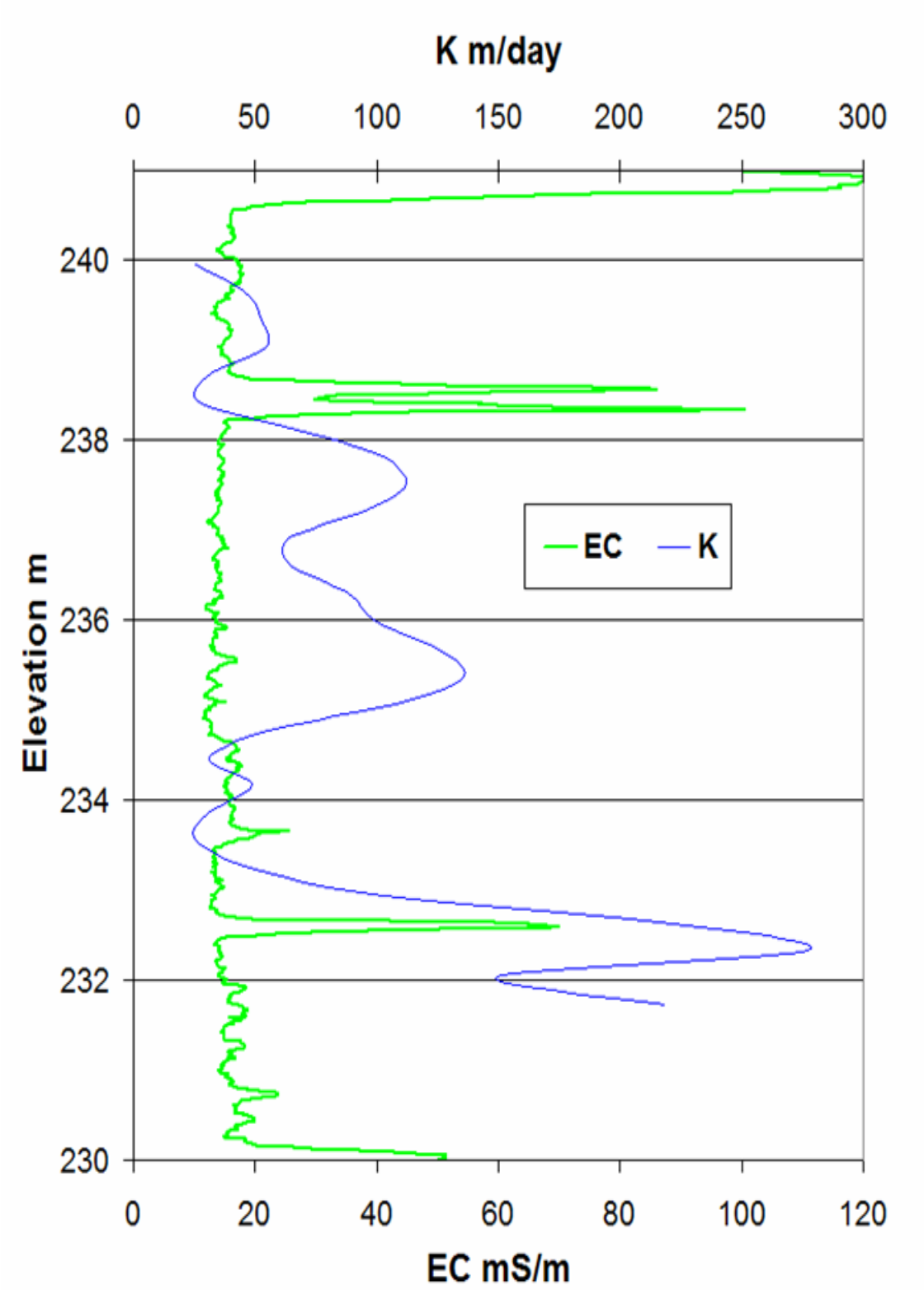

Figure A5. Well HT-2

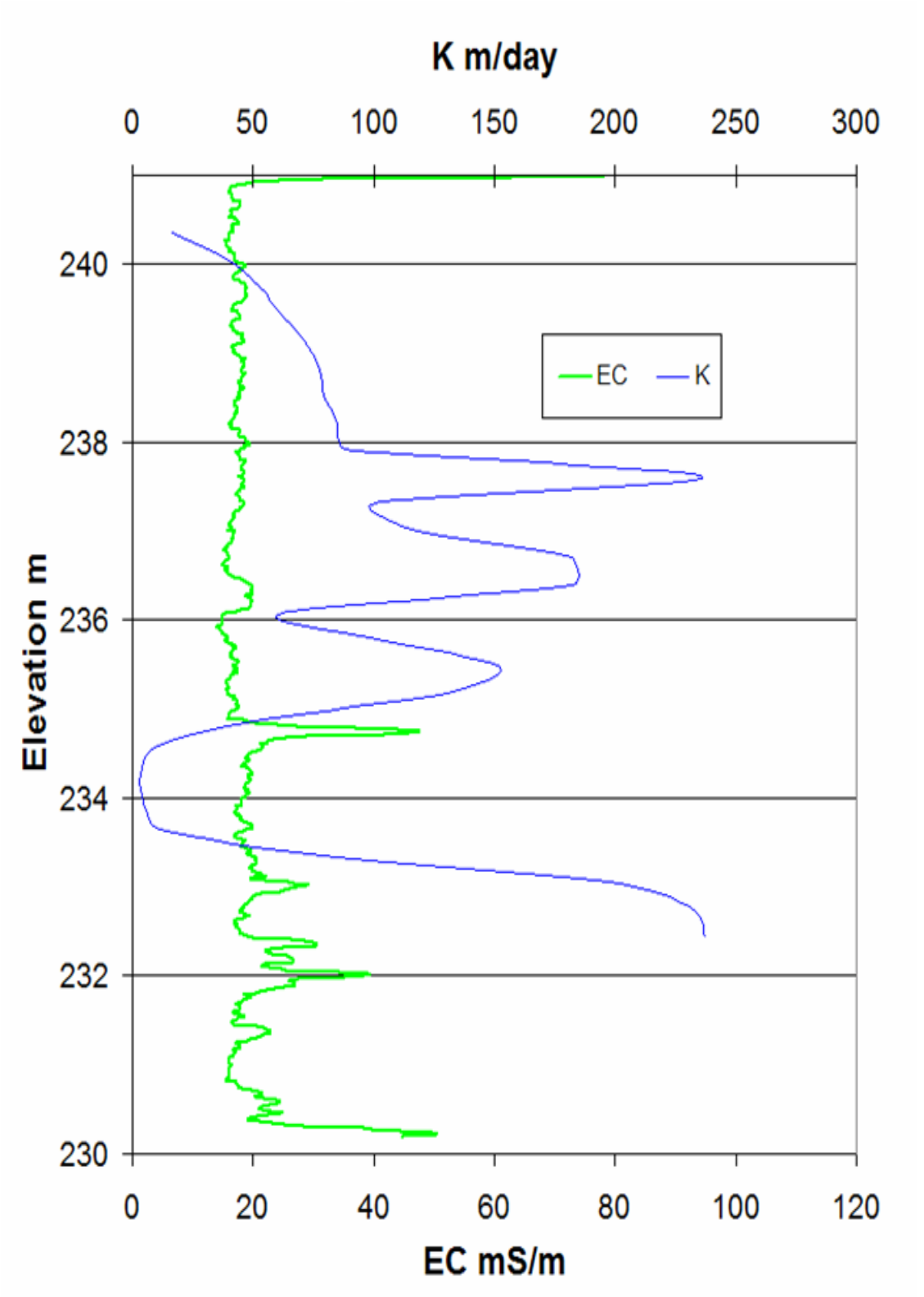

Figure A6. Well HT-3

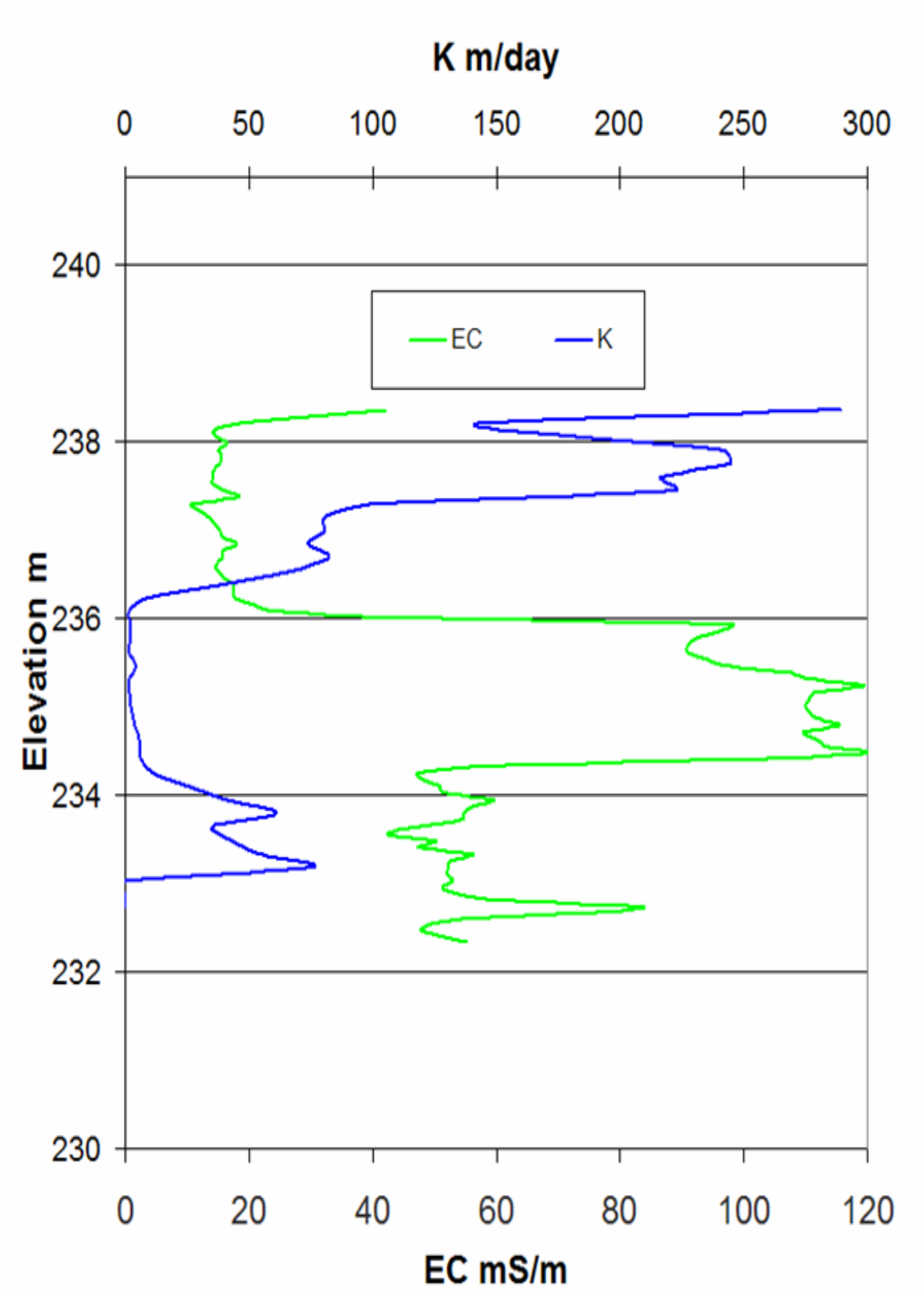

Figure A7. Well GEMS East

Appendix B. Comparison of phase shift and exponential (d) after correction for effective radius (r_o). **Figures B1 to B7 for line source data.**

Figure B1 **Well 00-3 to 7-1**

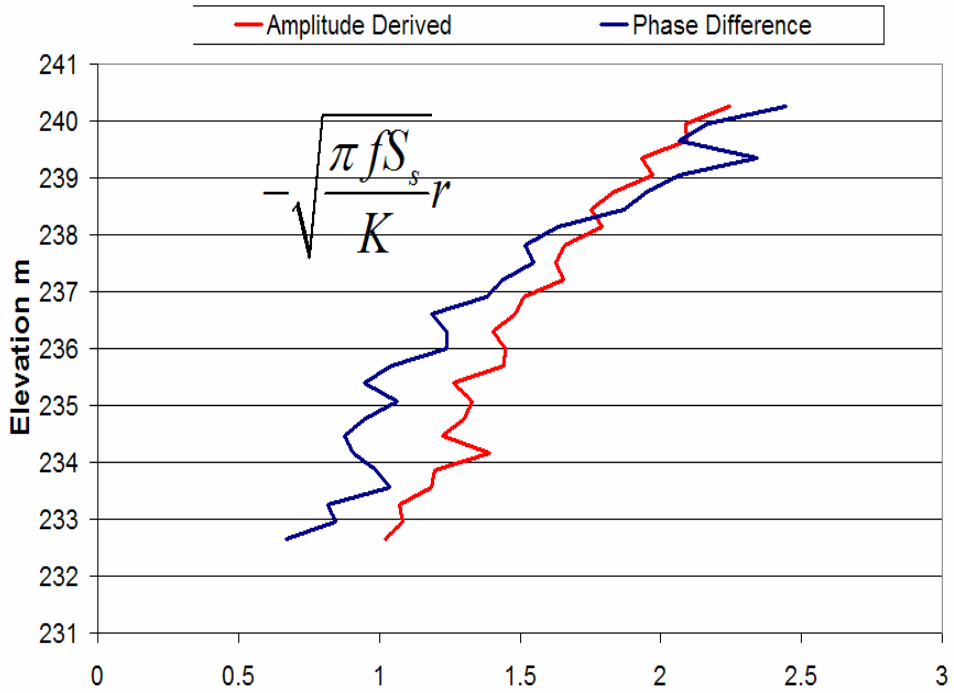

Figure B2 **Well 11-7 to 7-1**

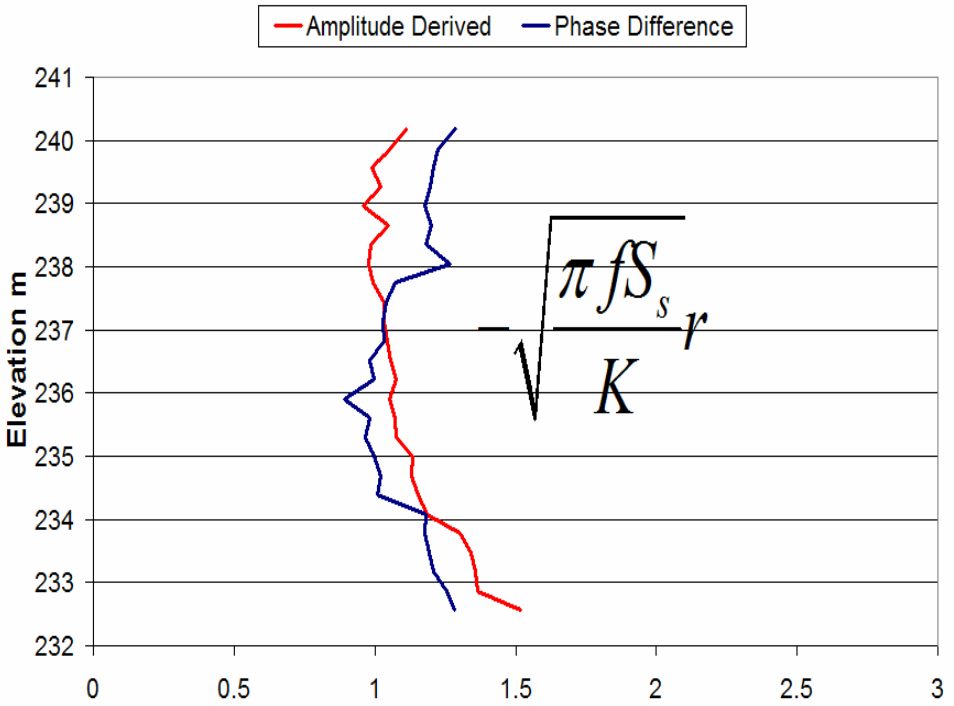

Figure B3 **Well HT-1 to 7-1**

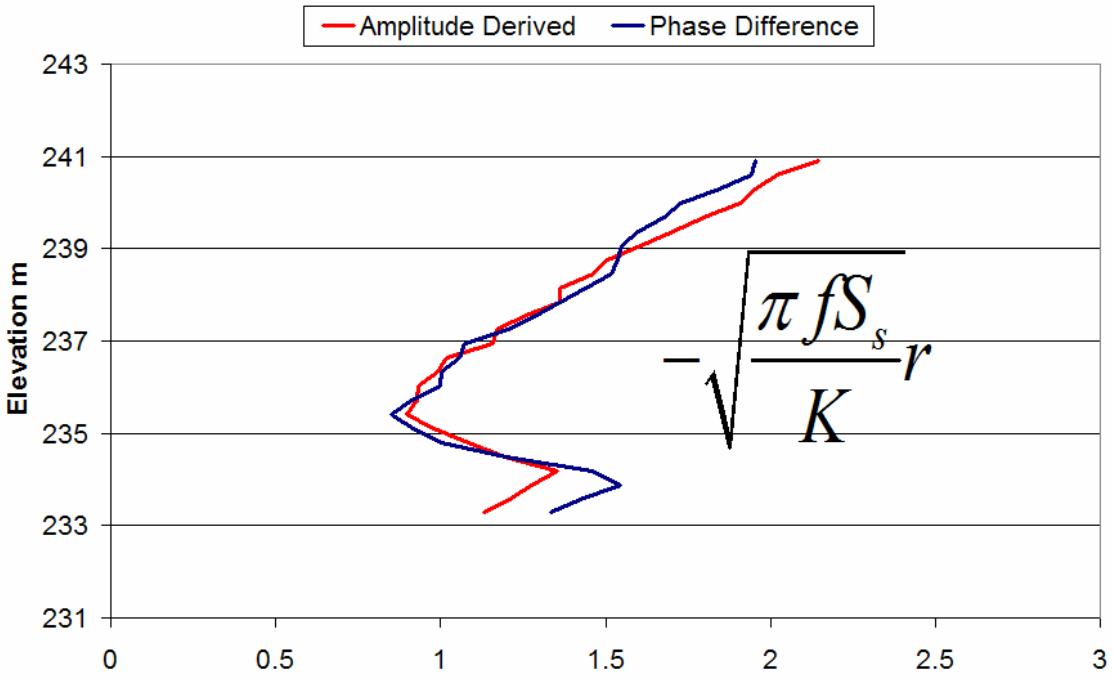

Figure B4 **Well HT-2 to 7-1**

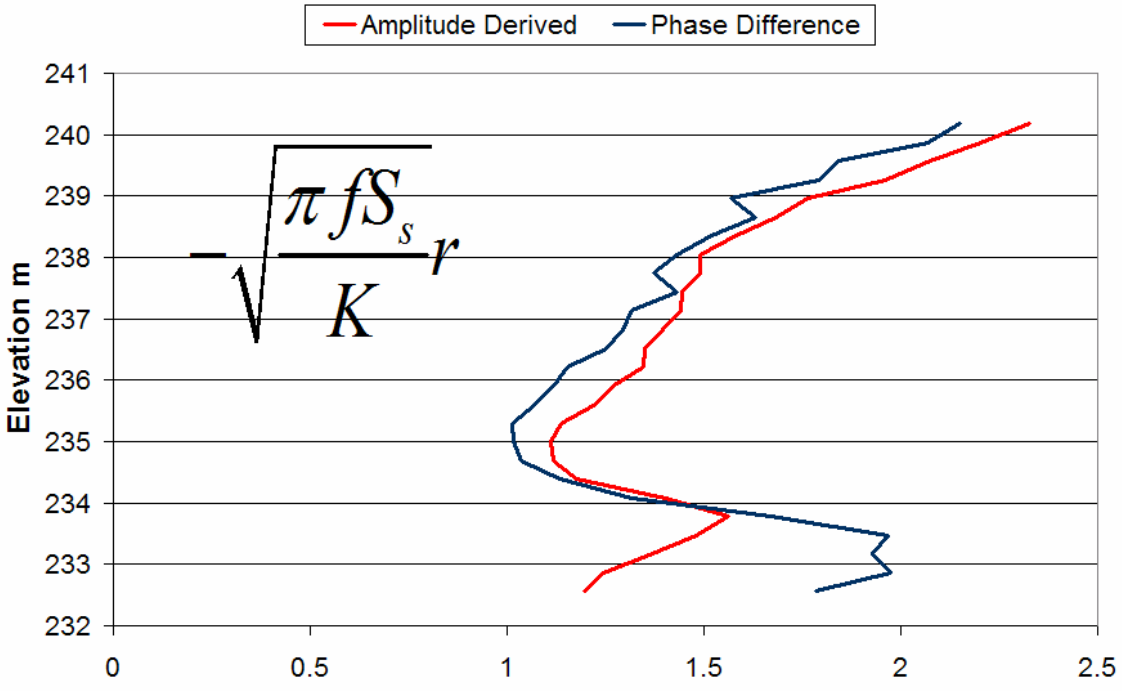

Figure B5 **Well 7-1 to HT-3**

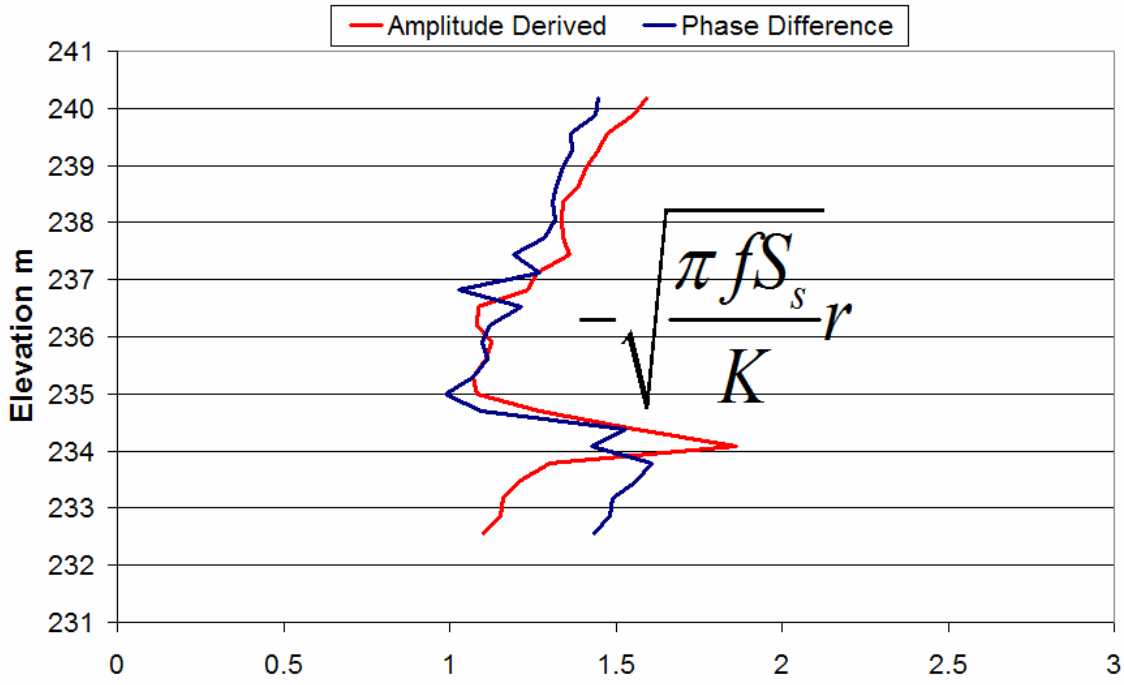

Figure B6 **Well HT-1 to HT-3**

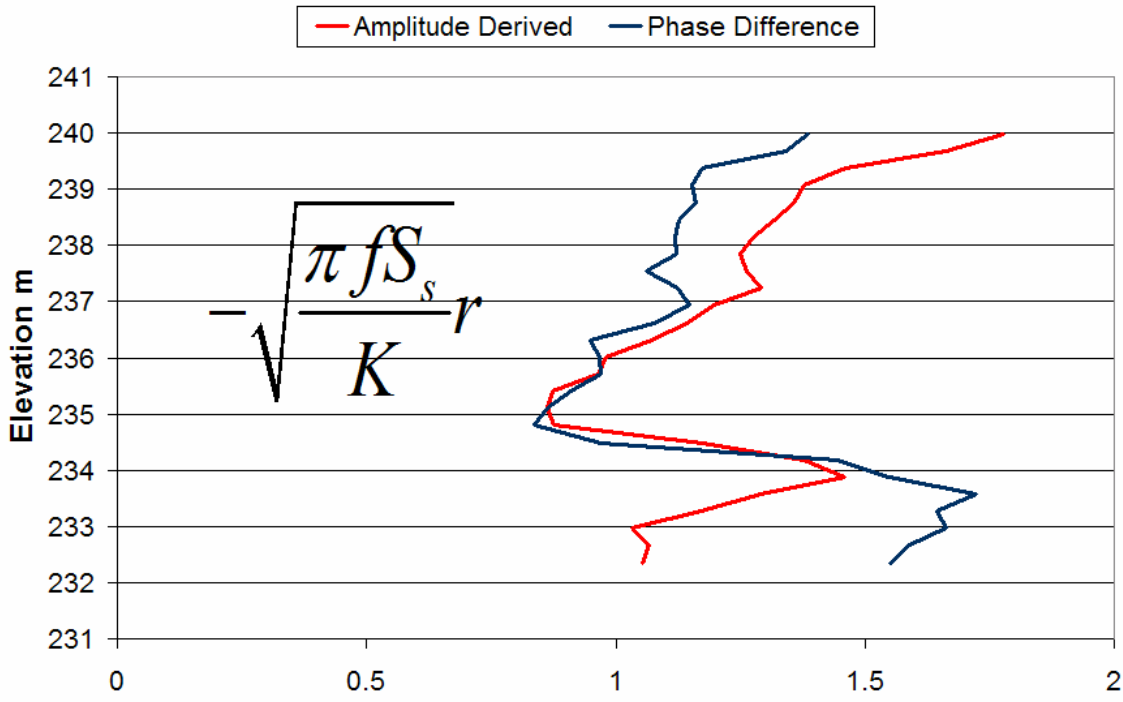

Figure B7 **Well HT-2 to HT-3**

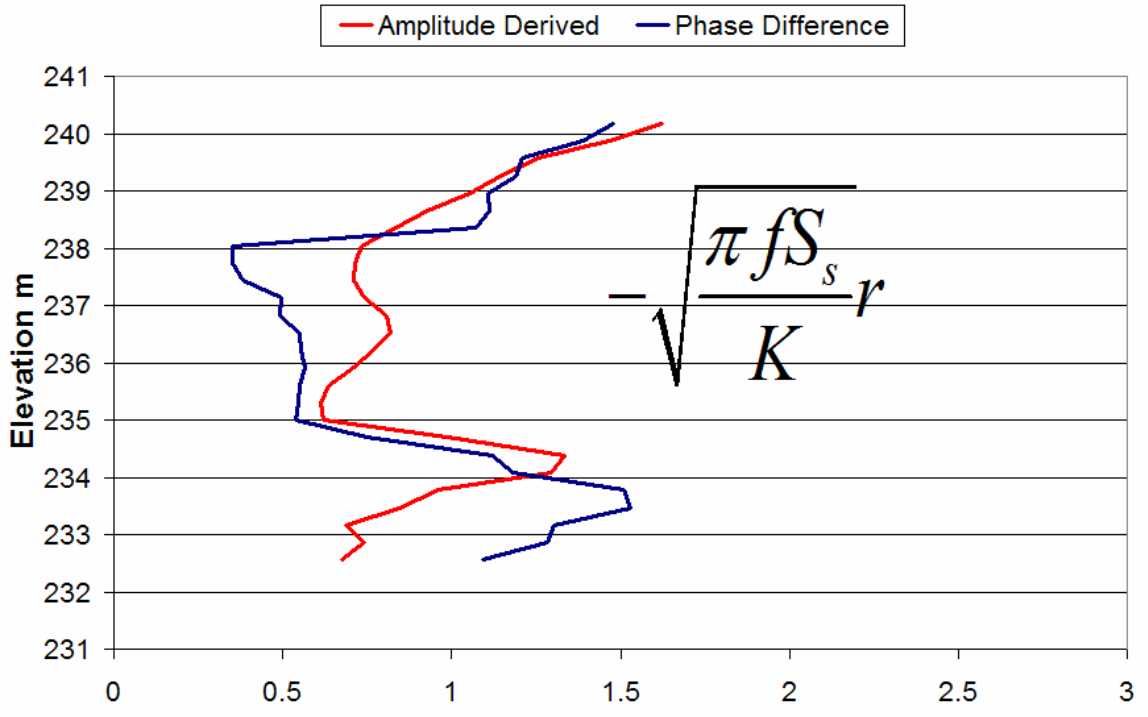

Figures B8 to B13 for point source data.

Figure B8 **Well 11-1 to 7-1**

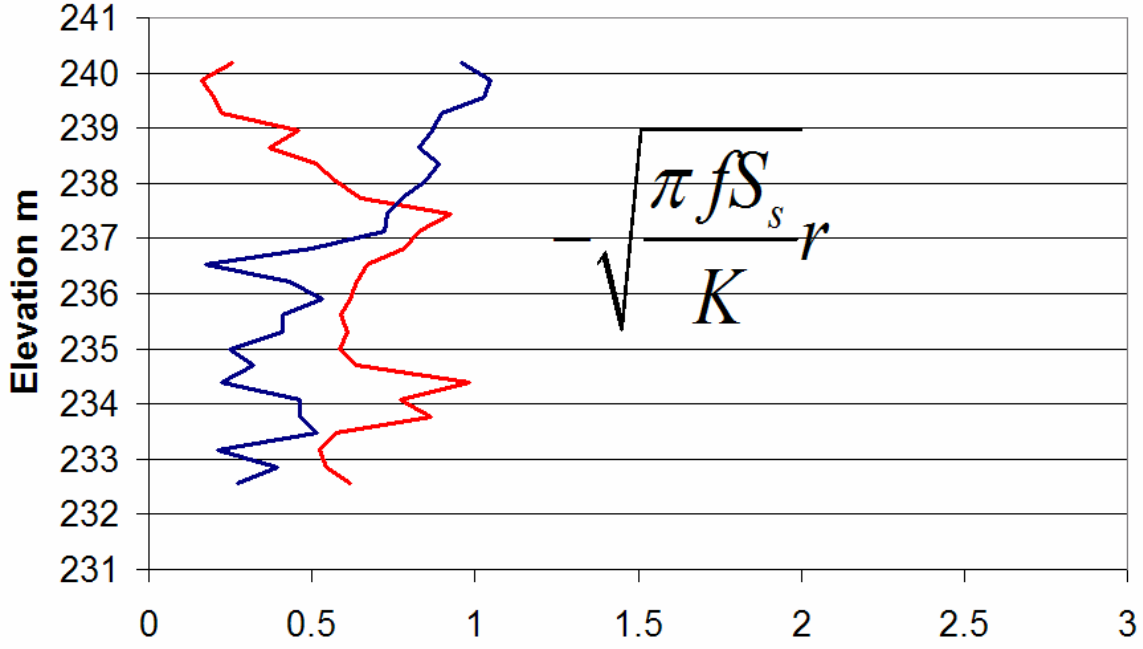

Figure B9 **Well HT-2 to 7-1**

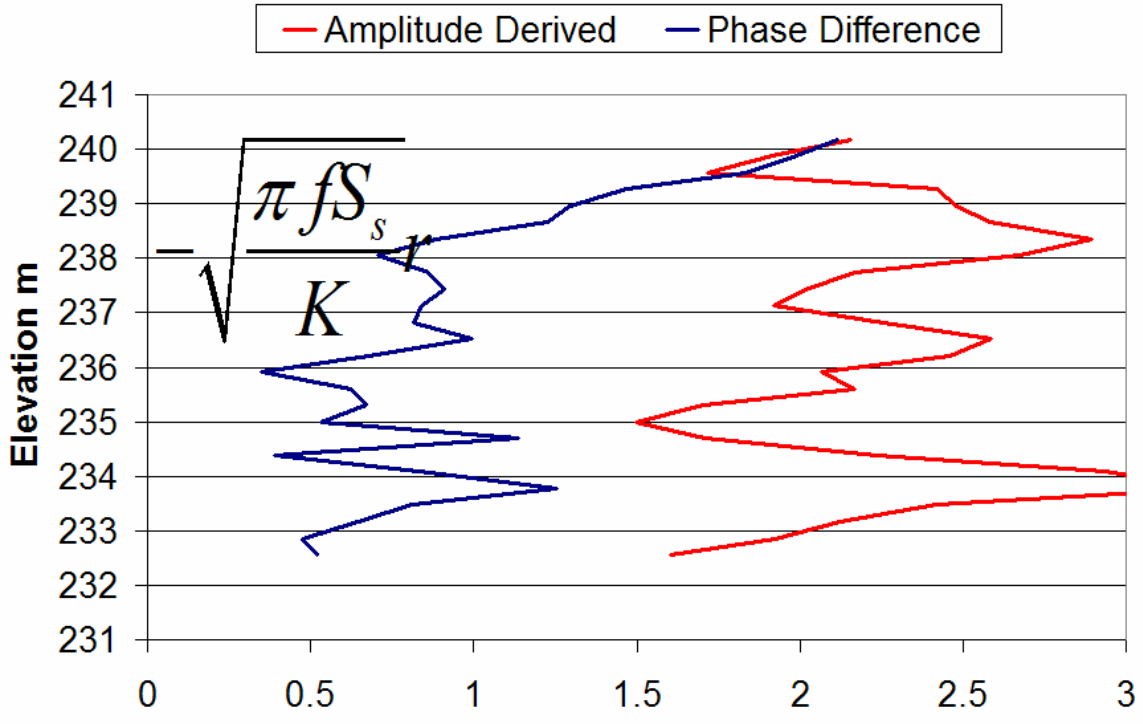

Figure B10 **Well 7-1 to HT-3**

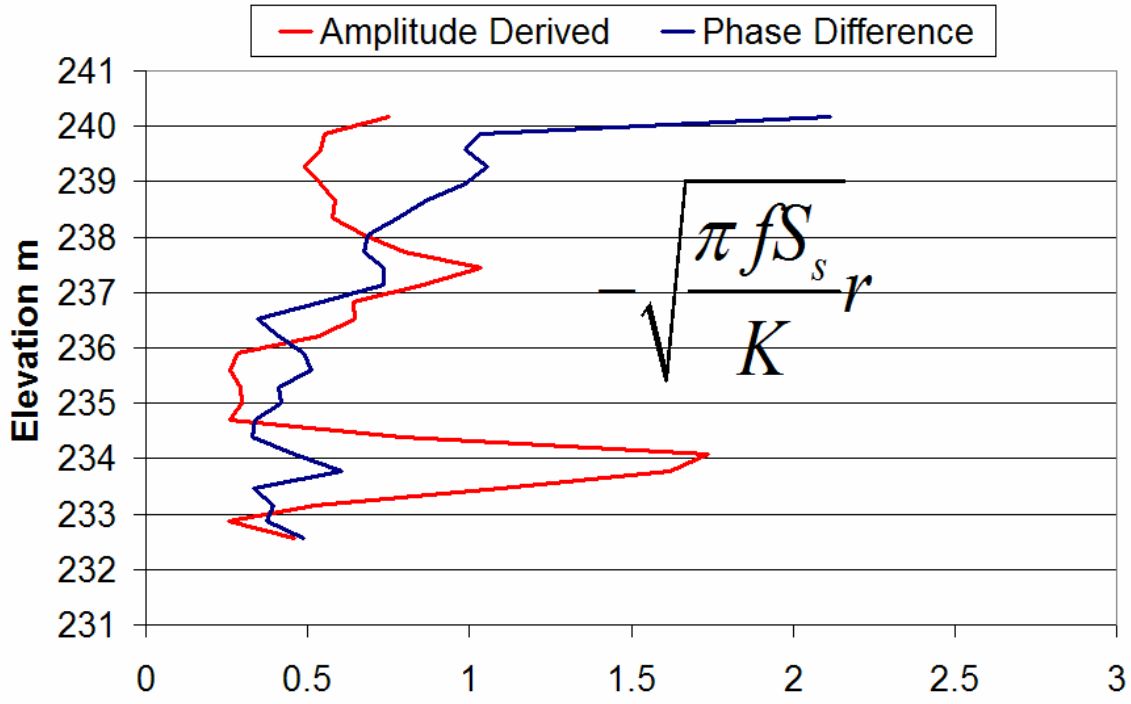

Figure B11 **Well HT-1 to HT-3**

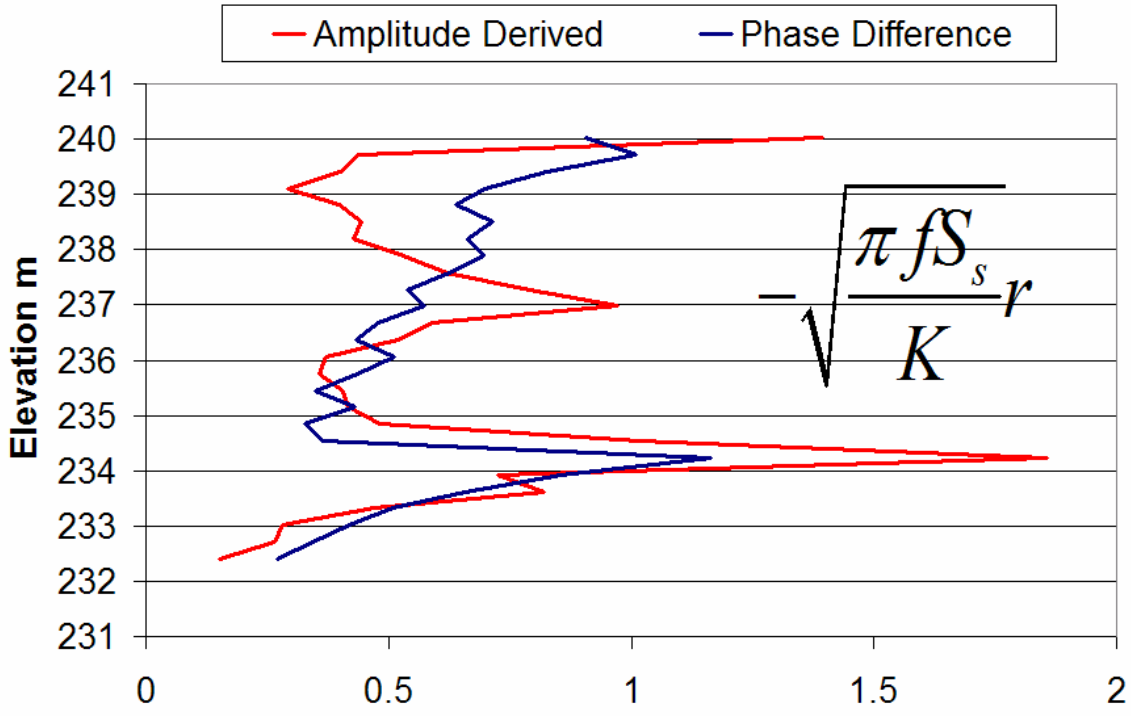

Figure B12 **Well HT-2 to HT-3**

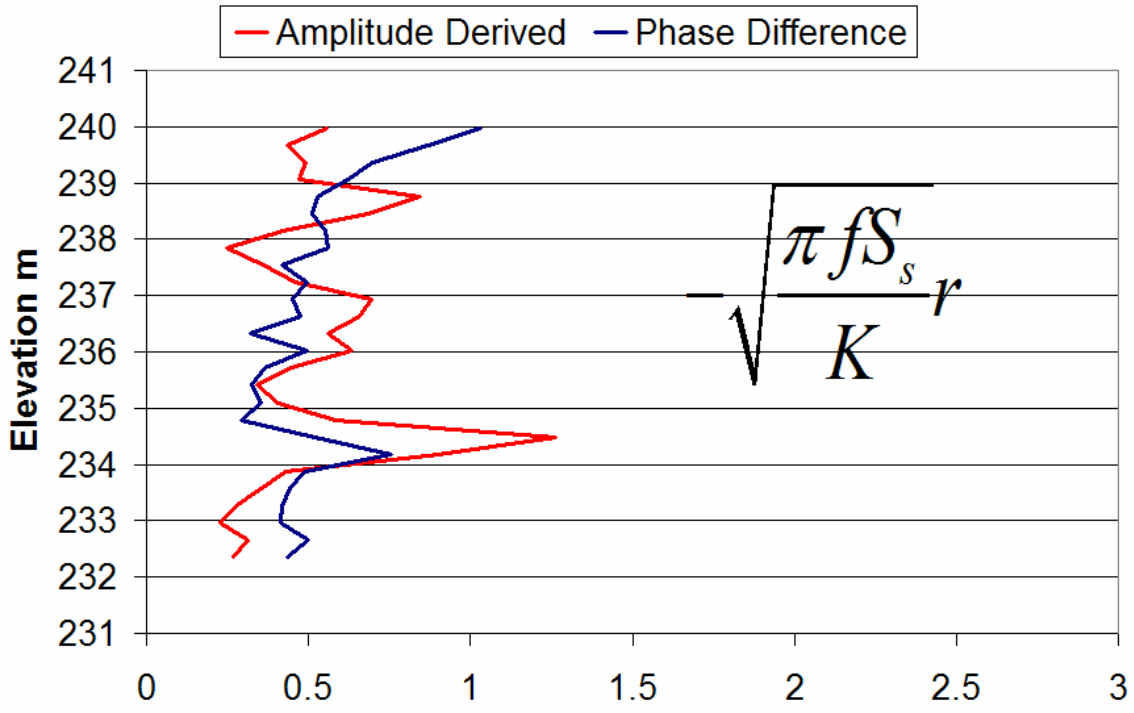

Figure B13 **Injection Well 11-1 to 7-1**

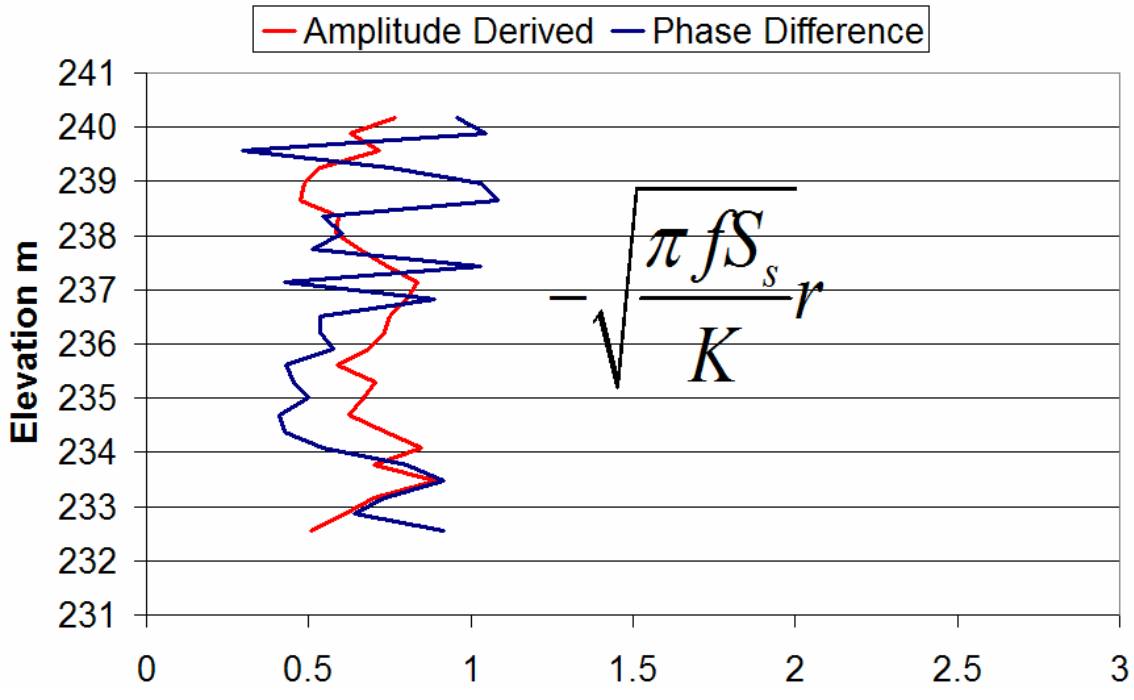

Appendix C. Presentation of phase, amplitude, and averaged K profiles from line source data compared to HRST K profiles.

Figure C1 Line Source Well 00-3 to 7-1

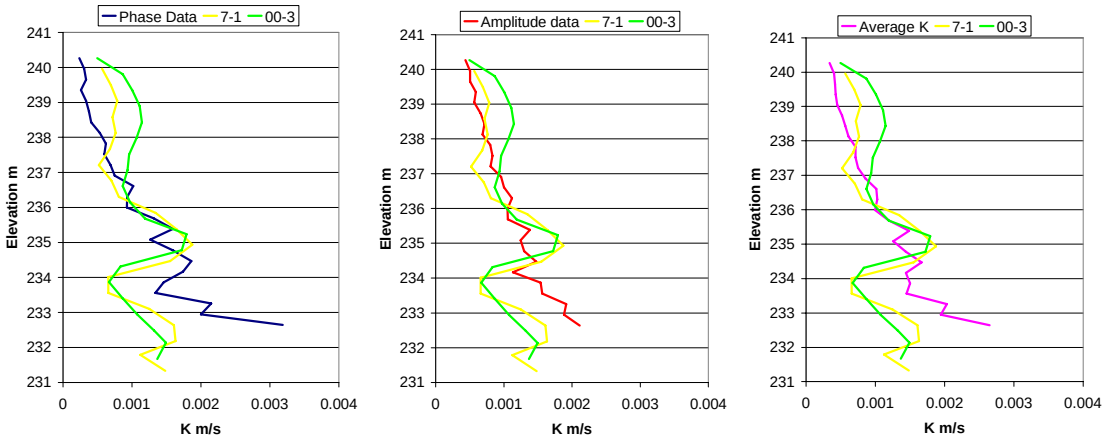

Figure C2 Line Source Well 11-1 to 7-1

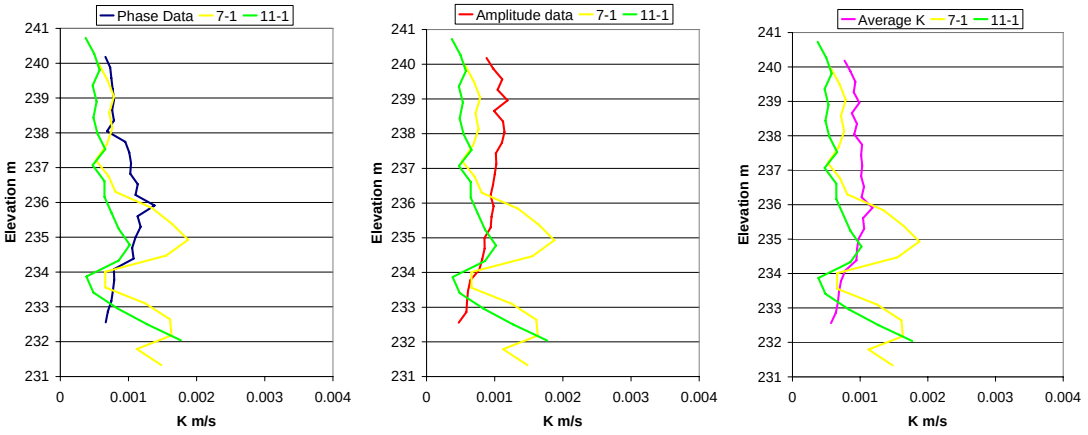

Figure C3 Line Source Well HT-1 to 7-1

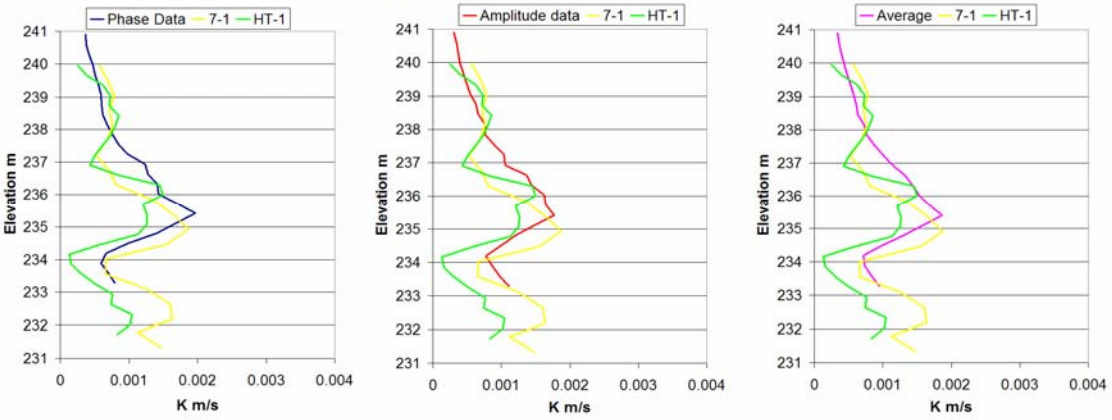

Figure C4 Line Source Well HT-2 to 7-1

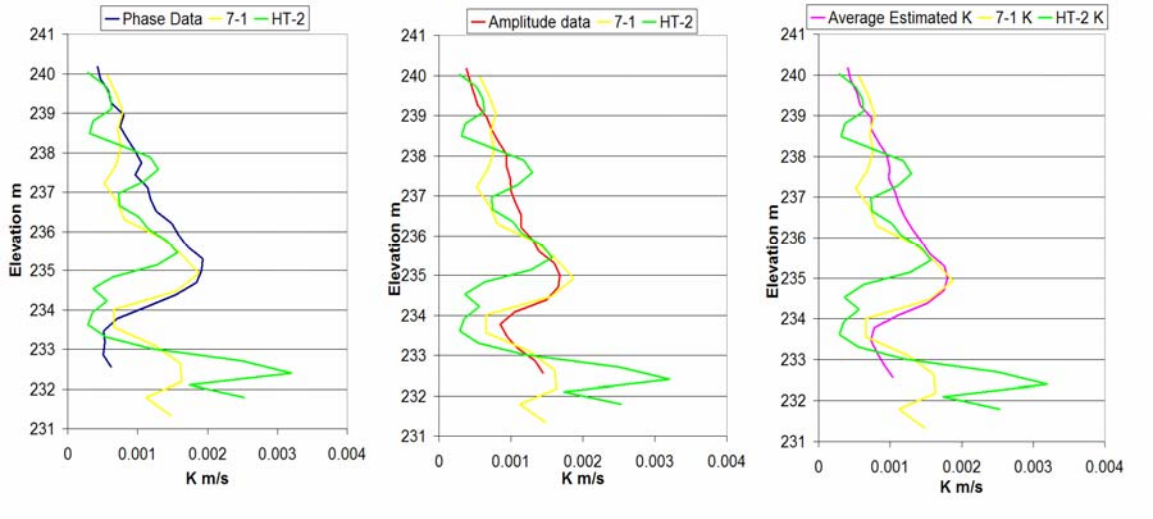

Figure C5 Line Source Well 7-1 to HT-3

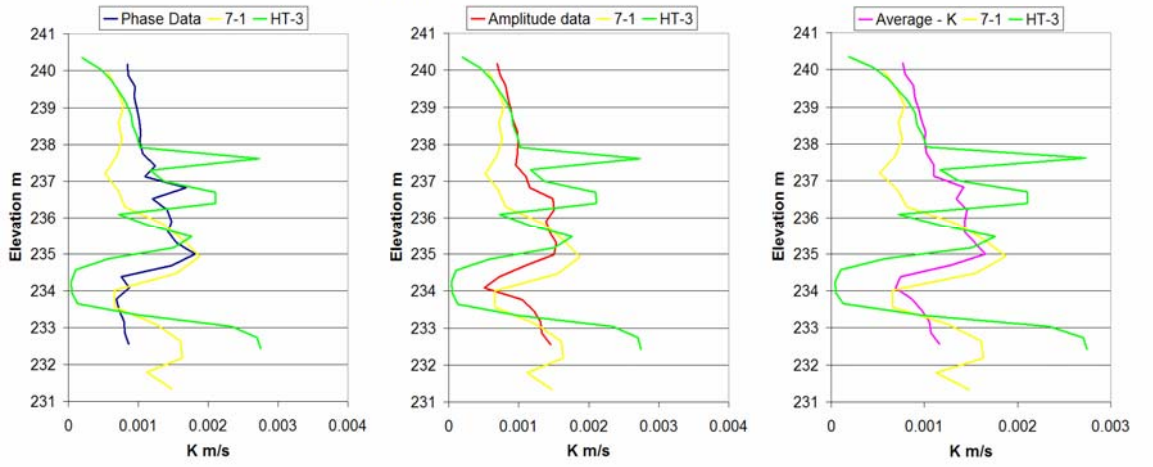

Figure C6 Line Source Well HT-1 to HT-3

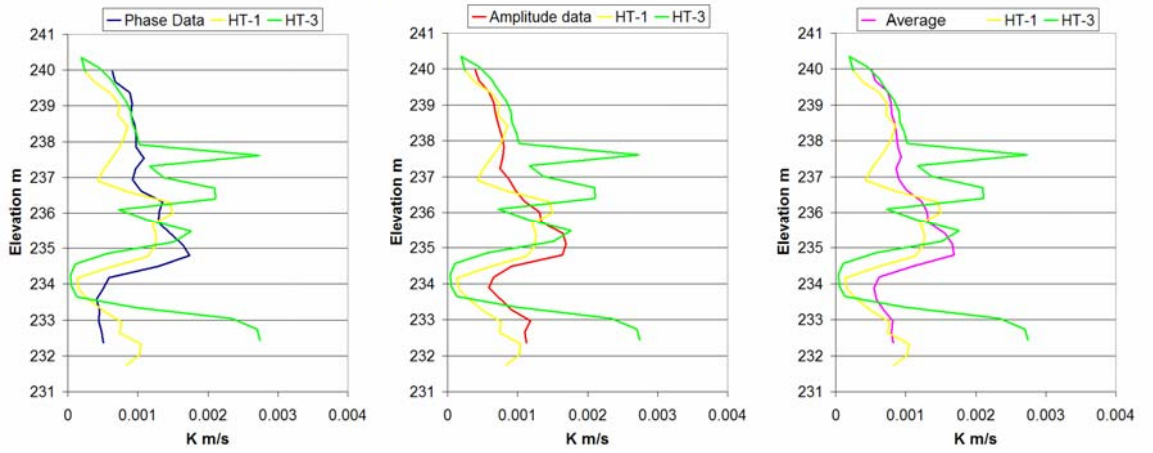

Figure C7 Line Source Well HT-2 to HT-3

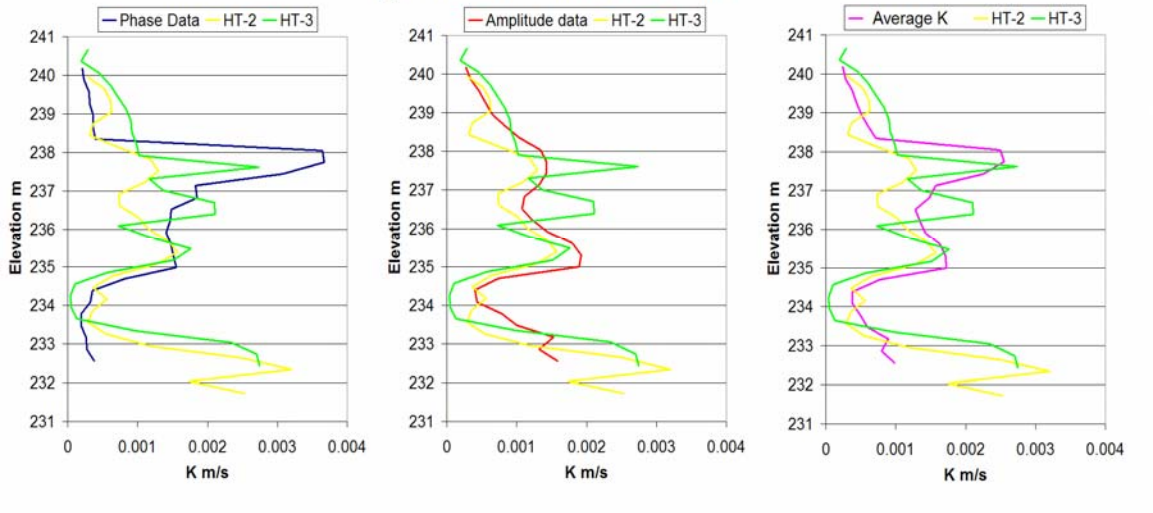

Appendix D. Presentation of phase, amplitude, and averaged K profiles from point source data compared to HRST K profiles.

Figure D1 Point Source Well 11-1 to 7-1

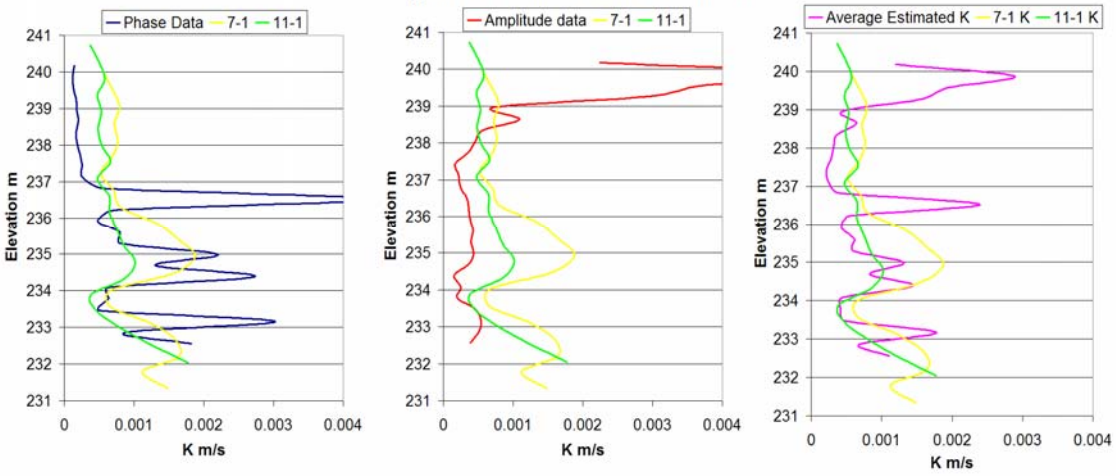

Figure D2 Point Source Well HT-2 to HT-1

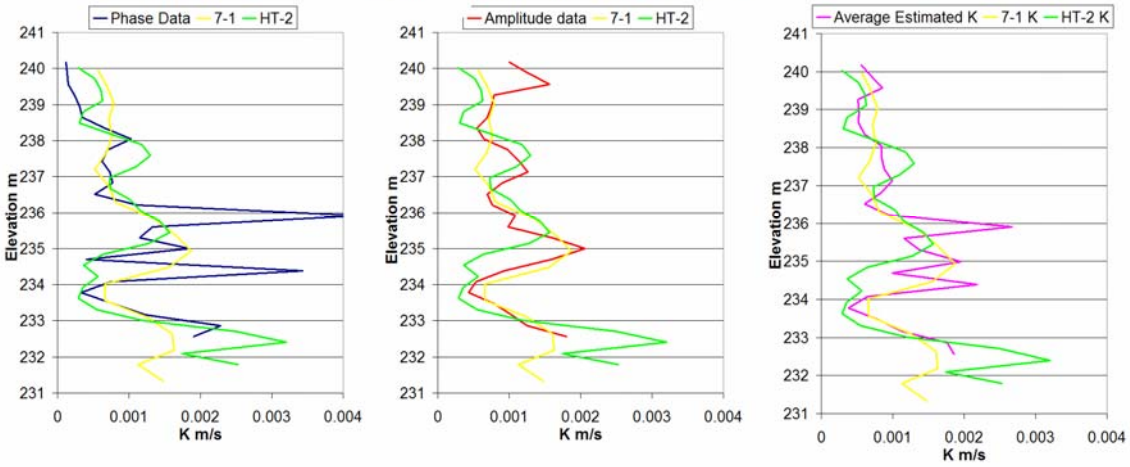

Figure D3 Point Source Well 7-1 to HT-3

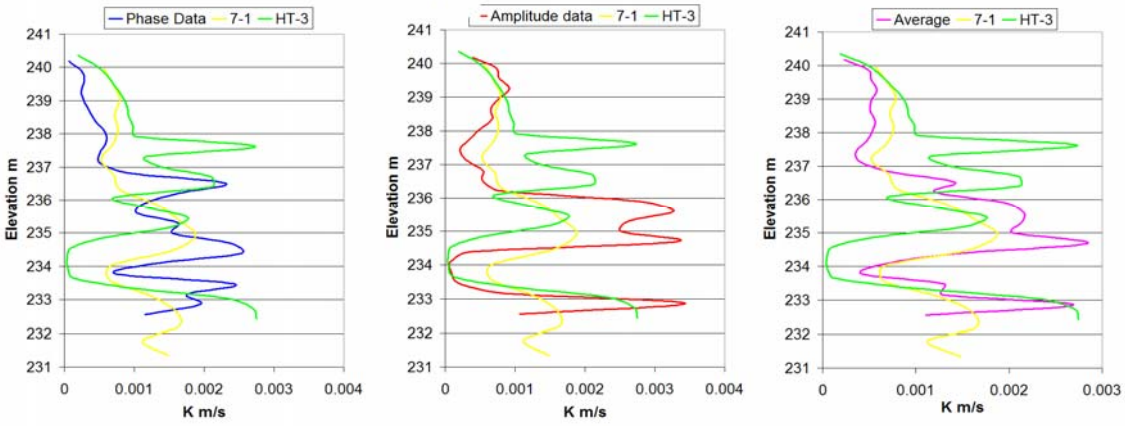

Figure D4 Point Source Well HT-1 to HT-3

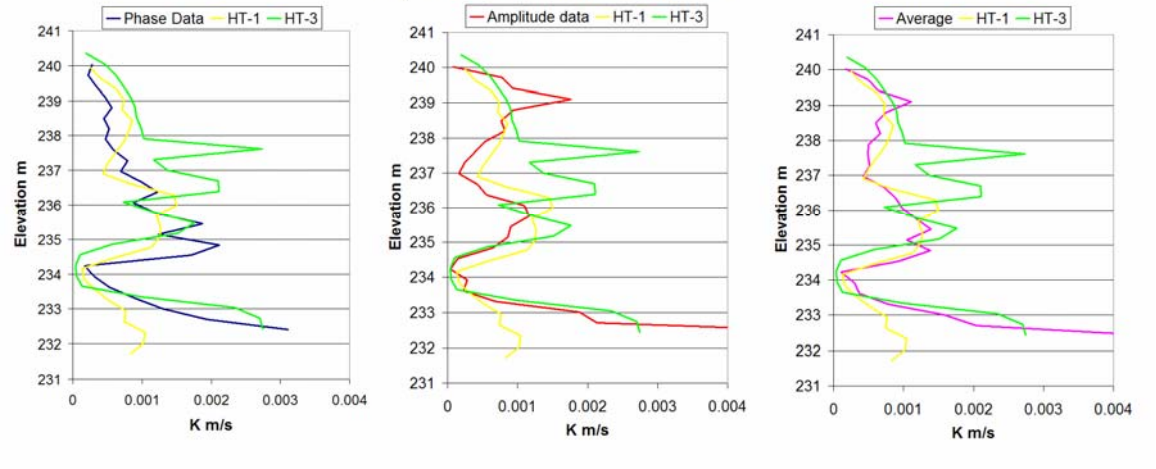

Figure D5 Point Source Well HT-2 to HT-3

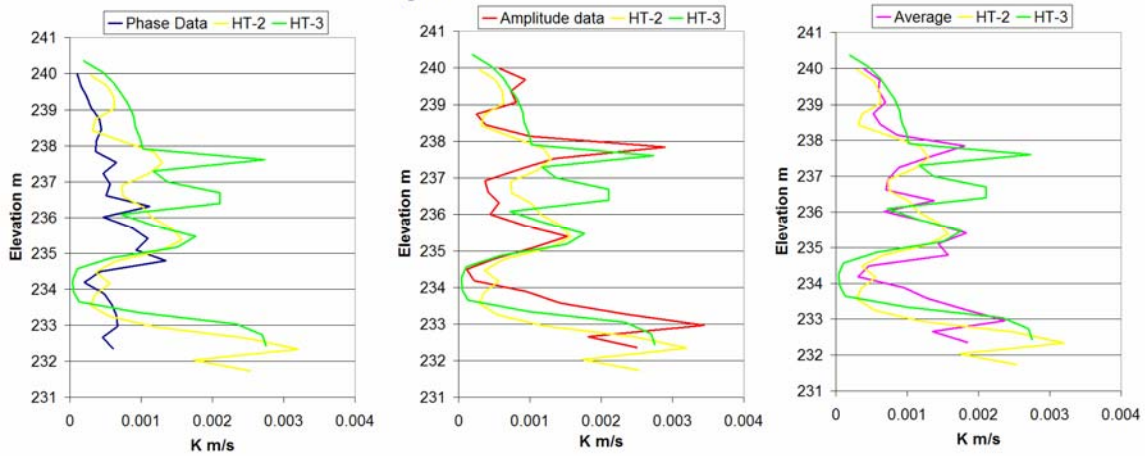

Figure D6 Injection Point Source Well 11-1 to 7-1

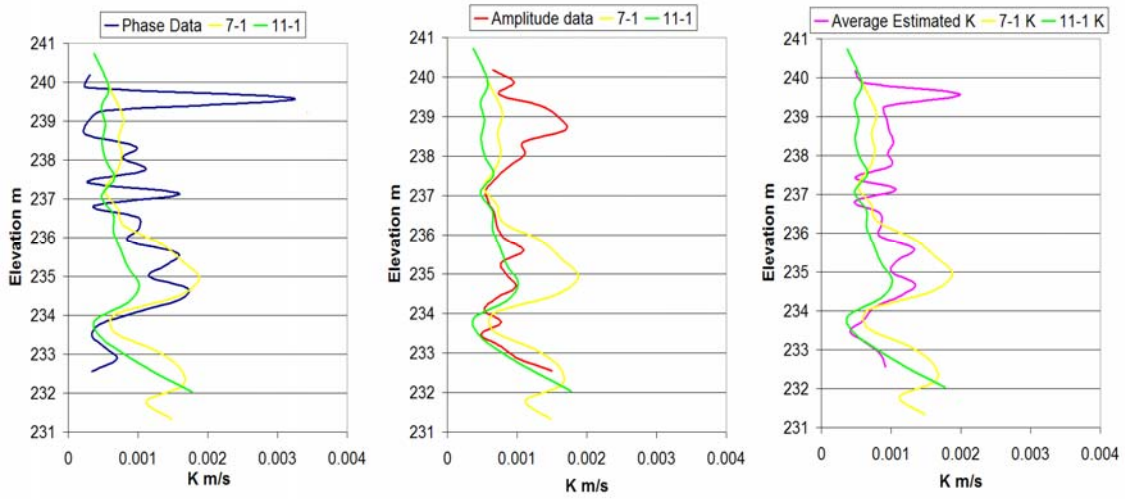

Appendix E. Technical Publications – Published Abstracts.

Healey, J. M., McElwee, C. D., and Engard, B., 2004, Delineating hydraulic conductivity with direct push electrical conductivity and high-resolution slug testing: *Eos, Trans. Amer. Geophys. Union*, v. 85, no 47, Fall Meet. Suppl., Abstract H23A-1118, p. F773.

Engard, B. and McElwee, C. D., 2005, Continuous pulse testing for estimating aquifer parameters: *Proceedings 50th Annual Midwest Ground Water Conference*, Nov. 1-3, Urbana, Illinois.

Engard, B. and McElwee, C. D., 2005, Estimating aquifer parameters from oscillatory well stresses: *Proceedings SERDP Partners in Environmental Technology Technical Symposium and Workshop*, Nov. 29-Dec. 1, Washington, D.C., p. G-26.

Engard, B. and McElwee, C. D., 2005, Estimating hydraulic conductivity: Hydraulic tomography and high-resolution slug tests: *Eos, Trans. Amer. Geophys. Union*, 86(52), Fall Meet. Suppl., Abstract H21C-1359.